12-2008

SYNTHESIS AND CHARACTERIZATION OF BIODEGRADABLE POLYURETHANES FOR BIOMEDICAL APPLICATION

Changhong Zhang
Clemson University, changz@clemson.edu

SYNTHESIS AND CHARACTERIZATION OF BIODEGRADABLE POLYURETHANES FOR BIOMEDICAL APPLICATION

A Dissertation
Presented to
the Graduate School of
Clemson University

In Partial Fulfillment
of the Requirements for the Degree
Doctor of Philosophy
Bioengineering

---

by
Changhong Zhang
December 2008

Accepted by:
Dr. Thomas Boland, Committee Chair
Dr. Andrew Metters
Dr. Ken Webb
Dr. Delphine Dean

ABSTRACT

This dissertation constitutes the studies about the biomedical materials research of novel polyurethanes. These elastic and degradable polyurethanes exhibited the potential for drug delivery, scaffold fabrication by novel ink-jet printing technology or other biomedical applications. This dissertation includes two parts about two different types of polyurethanes.

In the first part of this dissertation, we studied a polyurethane that was synthesized from methylene di-*p*-phenyl-diisocyanate (MDI), polycaprolactone diol (PCL-diol) and N, N-*bis* (2-hydorxyethyl)-2-aminoethane-sulfonic acid (BES). MDI, PCL-diol and BES were polymerized into polyurethane and served as the hard segment, soft segment and chain extender respectively. The effects of the chain extender BES on the degradation, mechanical properties, hydrophilicity, and cytophilicity of polyurethane were evaluated by comparison with the polyurethane that was chain extended by 2,2′-(methylimino)diethanol (MIDE).

In the second part of this dissertation, we studied a polyurethane synthesized from hexamethylene diisocyanate (HDI), polycaprolactone diol (PCL-diol), and a bicine chain extender. The chemical structure, mechanical properties, degradation rate, and swelling ratio were characterized by comparing the polymer with a polyurethane containing a 2,2′-(methylimino)diethanol (MIDE) chain extender. Due to the incorporation of negatively charged carboxyl side groups, the bicine extended polyurethane exhibited the environmental stimuli sensitivity, the polyurethane's

physical properties change in response to environmental stimuli, such as pH, ionic strength and temperature.

DEDICATION

This dissertation is dedicated to my family members and friends for their generous support.

ACKNOWLEDGEMENTS

I would like to express my gratitude to all those who gave me the possibility to complete this dissertation. I thank Professor Thomas Boland for his continuous guidance and support. I thank Professor Martine Laberge for her generous and unselfish assistance for my graduate study. I thank my other committee members, Dr. Ken Webb, Dr. Andrew Metters and Dr. Delphine Dean, for their helpful suggestions and comments throughout my PhD studies.

I thank the group members Mr. Nathan Brown and summer student Mr. Tianyi Hu for their support.

TABLE OF CONTENTS

LIST OF FIGURES

LIST OF TABLES

Chapter 1

DISSERTATION ROADMAP

Abstract

This dissertation constitutes the studies about the biomedical materials research of novel polyurethanes. The elastic and degradable polyurethanes exhibited the application for drug delivery, scaffold fabrication by novel ink-jet printing technology or potentials for other biomedical applications. This dissertation includes the synthesis and characterization of two different types of polyurethanes.

In the first part of this dissertation, we studied a polyurethane that was synthesized from methylene di-*p*-phenyl-diisocyanate (MDI), polycaprolactone diol (PCL-diol) and N, N-*bis* (2-hydorxyethyl)-2-aminoethane-sulfonic acid (BES), serving as a hard segment, soft segment and chain extender respectively. The effects of the chain extender BES on the degradation, mechanical properties, hydrophilicity, and cytophilicity of polyurethane were evaluated by comparison with the polyurethane that was chain extended by 2,2′-(methylimino)diethanol (MIDE).

In the second part of this dissertation, we studied a polyurethane synthesized from hexamethylene diisocyanate (HDI), polycaprolactone diol (PCL-diol), and a bicine chain extender. The chemical structure, mechanical properties, degradation rate, and swelling ratio were characterized by comparing the polymer with a polyurethane containing a 2,2′ -(methylimino)diethanol (MIDE) chain extender. Due to the incorporation of negatively charged carboxyl side groups, the bicine extended polymers exhibited the environmental stimuli sensitivity, whose physical properties change in response to environmental stimuli, such as pH, ionic strength and temperature.

Chapter 2

BACKGROUND

Introduction

Biocompatible polymers are extensively investigated for applications in tissue and organ repair. Among them, more and more studies are focused on using biodegradable polymers for tissue engineering purposes, because nondegradable polymers may become detrimental due to their impediment of graft-host integration, mechanical impingement, and long-term foreign body reactions [1-4]. Many different categories of biodegradable polymers, including both natural and synthetic, have been used for tissue repair purposes, such as collagen, chitosan, hyaluronic acid (HA), polyester, polyanhydride, polycarbonate, polyimide, polyamide, poly(amino acid), polyphosphazene, and so forth [5-14]. Although most of the currently investigated degradable polymers are well tolerated by cells in culture and in tissues, the mechanical properties of these polymers are not compatible with natural tissues. For example, most natural tissues, such as heart, blood vessels, skeletal muscle, tendon, and so forth, are very elastic and strong. The majority of degradable polymers are either too stiff/brittle with low elongation, or very soft with relatively low strength. With the increasing interest in engineering various tissues for the treatment of many types of injuries and diseases, a wide variety of degradable polymers with desirable mechanical, degradation, and cytophilic properties are needed. Because of its excellent mechanical properties and great chemical versatility [15-22], elastic degradable PU shows promise as being a good candidate for most soft tissue regeneration, such as cardiac muscle [23], blood vessel [19, 24], skeletal muscle,

tendon, ligament, and skin repair. In addition, elastic degradable PU is also investigated for hard tissue regeneration, such as cartilage [22], bone tissue repair [21, 25] and drug delivery system [26, 27]. The majority of investigations in the past were focused on the development of nondegradable PUs for long-term implantation, such as pacemaker lead insulators, catheters, cardiovascular grafts, and so forth [28]. Relatively few investigations had been directed toward developing degradable PUs [15-25, 29-33]. In this chapter, we briefly review the PU chemistry, design of the degradable PUs, current research of the degradable PUs and the action of PUs on inflammatory cells. It may help our understanding of the biodegradable PUs in biomedical application and direct us to develop the functional biodegradable PUs for biomedical uses.

Polyurethanes (PUs) chemistry, structure

Polyurethane is a general name of a family of synthetic copolymers that containing the urethane moiety (as shown in Figure 1) in their chemical repeat structure. As a family of biomaterials, PUs are most frequently synthesized as segmented block copolymers.

Figure 1: Illustration of urethane linkage

The segmented PUs can be represented by three basic components in the following general form:

$$\mathbf{P\text{-}(D(CD)_n\text{-}P)_n}$$

Where P is the polyol, D is the diisocyanate and C is the chain extender. Typically, the polyol, or the so-called soft segment, is an oligomeric macromonomer comprising a 'soft flexible' chain having a low glass transition temperature (less than 25 ^{o}C) and terminated by hydroxyl (–OH) groups. The chain extender is usually a small molecule with either hydroxyl or amine end groups. The diisocyanate is a low molecular weight compound that can react with either the polyol or chain extender, leading to the interesting segmented structure illustrated above. The combination of the chain extender and the diisocyanate components is referred to as the hard segment of the polymer. In linear PUs, all the three components have a functionality of two, if a branched or crosslinked material is desired, multifunctional polyols, isocyanates, and sometimes chain extenders can be incorporated into the formulation.

The principle chemical reaction involved in the synthesis of PUs is the formation of prepolymer through urethane-forming reaction, as shown in Figure 2.1.2a, the reaction between isocyanate and hydroxyl groups. Because this is the nucleophilic addition reaction, it is catalyzed by basic compounds such as tertiary amines and by organic metal compounds such as organotin. Another important basic reaction in PUs synthesis is the chain extending reaction for the prepolymers, which occurs between chain extender (diol or diamine) and isocyanate group on the prepolymer. When a diol is used as chain extender, urethane will be formed according to Figure 2a, while urea will be formed according to Figure 2b if diamine is used for chain extending reaction.

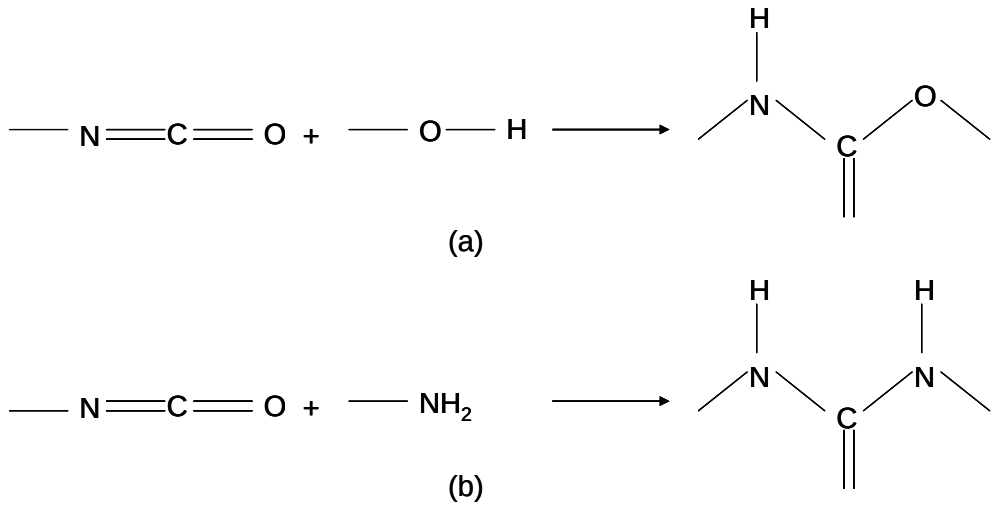

Figure 2: Chain extending reaction occurs between chain externder and isocyanate. (a) the reaction between diol and isocyanate group, urethane will be formed; (b) the reaction between diamine and isocyanate group, urea will be formed.

Therefore, the traditional synthesis of linear PU includes prepolymer synthesis reaction, followed by chain extending reaction. During the laboratory synthesis of PU, solvent is usually used to reduce the viscosity and promote the formation of high molecular weight copolymers. This polymerization often follows the two-step procedure: first, an isocynate end-capped prepolymer is formed by the reaction of polyol with excess diisocyanate; then the chain is extended to high molecular weight through the reaction of residual isocyanate functionality with added chain extender. Commercial PUs are usually prepared without solvent either by a similar two-step procedure forming first the prepolymer or by the so-called “one-shot” process in which all three monomers are mixed simultaneously. Alternatively, bulk polymerization can be accomplished by reaction injection molding (RIM), in which a stream of diisocyanate and one of polyol with chain extender is rapidly combined by impingement mixing directly before entering a mold cavity. Because the segmented PU is composed of three raw material reactants:

polyol, diisocyanate and chain extender (diamine or diol). The final properties of the PU are mainly dependent on the chemical and physical nature of these three building segments.

The conventional polyols are usually polyethers (with a repeating structure of –R–O–R'–) or polyesters (with repeating structure of –R–CO–O–R'–), with chain ends terminated by hydroxyl groups. Polyols can be liquid or solid (wax-like), depending on the molecular weight. Due to their aliphatic structure and low intermolecular interaction, particularly the abundant ether bonds, polyol molecules rotate and bend easily and are therefore soft materials. Consequently, the polyol sequence of PU is referred to as the soft segment.

The most important isocyanate used in PU manufacture is diisocyanate, containing two isocyanate groups per molecule. These two functional groups work to join together by chemical reaction with two other molecules (polyol or chain extender) to form a linear chain. Diisocyanate can be either aromatic or alilphatic. When the functionality is greater than two, a branch site is formed between the molecules, leading to network or crosslink formation.

Because the direct reaction of polyol with diisocyanate groups produces a soft gum rubber with poor mechanical properties, the chain extender is needed to drastically improve the final product mechanical strength. The role of the chain extender is to produce an 'extended' sequence in the copolymer consisting of alternating chain extender and diisocyanates. These extended sequences, or hard segments, act both as filler particles and physical crosslink sites to increase mechanical strength. Two commonly

used chain extender in industry is butane diol (BD) and ethylene diamine (ED). However, in lab research, other chain extenders were taken into consideration to obtain different PUs with specific functionality.

PU laboratory synthesis

The laboratory synthesis of PU is usually carried out in a three-neck glass flask and a common set-up is illustrated in Figure 3. The inlet has three functions: connection to vacuum line, introduction of nitrogen gas, and adding reactants. The speed of reactant addition needs to be regulated. The reaction should be performed under nitrogen atmosphere in order to protect from moisture and oxygen. Efficient stirring is very important to ensure uniformity of the reaction and a narrow distribution of molecular weight, particularly in the chain extension step. In the classic two-step solution phase synthesis of PU composed of MDI, PTMO and BD, the following procedures are commonly adopted [34]:

1. Set-up of the reactor according to Figure 3. Glassware is recommended to be predried, the reactor is vacuumed and then purged with nitrogen gas. A slight positive nitrogen pressure is kept in the reactor by connection of the reactor with a balloon inflated with nitrogen gas.

2. Preparation of the reactants. It is strongly recommended that all of the reactants be purified before the synthesis. Polyol should be dried with strong agitation at 100-120 ^{o}C under vacuum for few hours to ensure the water content is less than 0.03%. Distillation can be used to purify the chain extender and the isocyanate. The distillation

of isocyanate should be carried our under reduced pressure to avoid the self-addition reaction of isocyanates at elevated temperature. Solvent should also be freshly distilled or treated with metallic sodium to remove traces of water.

3. Adding isocyanate compound to the reactor. The temperature of the reactor is kept at a predetermined temperature.

4. Adding polyol to reactor. The polyol should be slowly introduced under constant agitation. Once the addition is completed, the reaction is maintained at 70-90 ^{o}C with agitation for 2-3 hours to complete the reaction.

5. Predetermined amount of purified solvent is added to the reactor. The temperature of the reactor is reduced to 40-60 ^{o}C. The solvent will reduce the viscosity of the PU and maintain effective agitation in the next chain-extending step. The amount of solvent can be calculated based on the desired final concentration of the PU solutionm for examples, 20% wt/v.

6. Adding chain extender. Chain extender should be slowly added under vigorous agitation. The reaction is kept between 0-100 ^{o}C according to the chain extender properties until completion. At this stage, significant increase of viscosity and temperature will be noticed and efficient agitation is extremely important. Completion of the reaction is indicated by the attainment of constant viscosity or by the residual isocyanate index.

7. Terminate of the reaction by introducing chain-terminating agent such as methanol.

8. Store the PU solution in dark-colored container and preferably under sub-ambient temperature; or dump the solution into plenty of de-ionized water to precipitate the polymer, the polymer was put in the water for several days for purification of the impurities, and then vacuum dried below 60 ^{o}C.

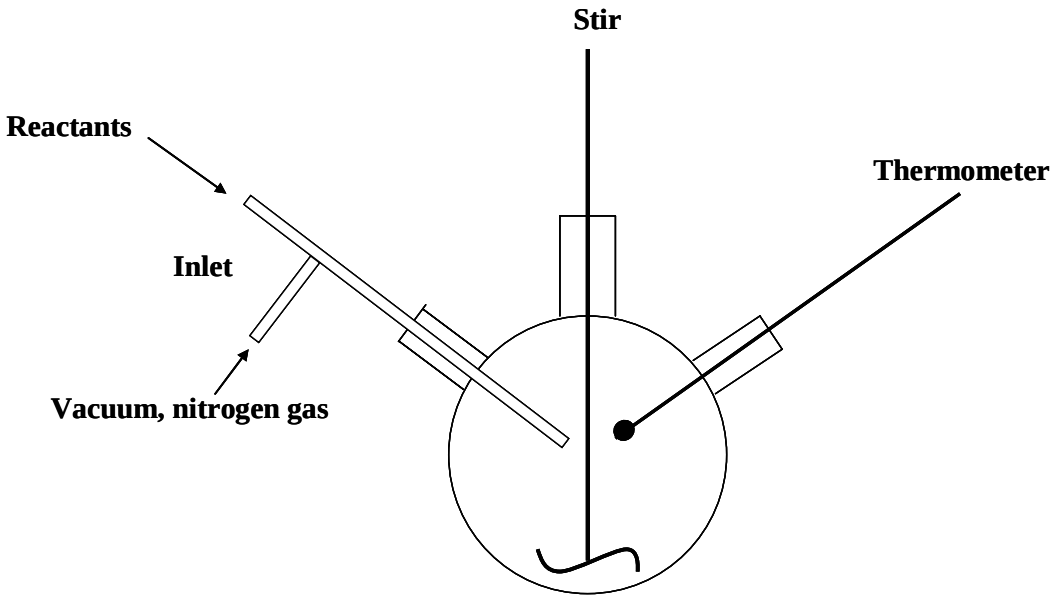

Figure 3: Laboratory set-up for the synthesis of PUs.

Selection of segments for biodegradable PUs

As of the choice of PU hard segment, typically, an aromatic diisocyanate was employed for applications where degradation was not desired, such as pacemaker lead coverings, catheters, and wound dressings [35]. Due to the putative carcinogenic nature of aromatic diisocyanates [36, 37], degradable PUs are most frequently made from

aliphatic diisocyanates such as lysine diisocyanate (LDI) [38], hexamethylene diisocyanate (HDI) [39] and 1,4 diisocyanatobutane (BDI) [40], whose degradation products are more like to be non-toxic, i.e. lysine, 1,4-butanediamine (putrescine), etc. But methylenebisphenyl isocyanate (MDI) was still in use in the lab research for the PU synthesis due to its high chemical reactivity and rigidity, which can enhance the final PU products tensile strength due to the strong tendency of rigid aromatic moieties to pack efficiently. Because of the presence of hydrogen bonding between isocynate-derived groups (urethanes and ureas), isocyanate segments tend to self-organize to form semi-crystalline phases within the polymer macromolecular assembly. Each type of diisocyanate has a different intrinsic ability to form such microphase structures. As the elasticity of the polymers depends on their degree of crystallinity and degree of hard segment segregation, it is clear that the selection of the diisocyanate monomer will be one of the key parameters that influence PU mechanical characteristics. Briefly, PUs containing aromatic diisocyanate, such as MDI and phenyl diisocynate (PDI), are more rigid than those containing aliphatic diiscynante such as BDI, HDI, LDI as mentioned above.

The soft segment is typically the block of the PU used to modify the degradation rate, thus biodegradable PUs have been made with a variety of soft segments including polylactide or polyglycolic acid [41], polycaprolactone (PCL) [42], polyethylene oxide [43], glycerol and/or sucrose [44, 45] . To date, the most efficient and applicable way to control the degradability of PUs were by changing the soft segment component. Commonly, polycaprolactone diol (PCL) and/or polyethylene glycol (PEG) with different

molecular weight were selected to synthesize linear or crosslinked PU. PCL and PEG impart different physical properties such as mechanical strength, hydrophilicity and degradability to the PUs contain them. For example, PEG is used to enhance degradation and PCL to provide greater hydrolytic stability and electrometric mechanical properties. PCL usually imparts enhanced crystallinity to the PU while PEG increased hydrophilicity and water uptake. PU with higher molecular weight PCL exhibits higher degradation rate and unchanged hydrophilicity compared to the PU with lower molecular weight PCL, while PU with higher molecular weight PEG exhibits higher hydrophilicity.

Although chain extender is generally with low molecule weight, its chemical structure can also have a profound influence on the physical and biological properties of PUs. In some study [42], a slightly structure difference of the chain extender butane diol (BD) and methylimino diethanol (MIDE) caused dramatically change of the PU's degradation, mechanical properties, hydrophilicity and cytophilicity. By changing chain extender, enzyme sensitive linkage can be introduced into PU and the enzymatic degradation can be employed [46, 47].

Degradation of PUs in biomedical devices

Generally, the degradation of PUs in tissue environment follows bulk degradation mechanism. Once PUs were implanted, there are several factors were contributed to their degradation, including hydrolysis, stress cracking, oxidation and enzymes. For example, the aliphatic ester linkages in polyester-urethanes are easy to be hydrolyzed into small molecules [48]. And polyether-urethane material are known to be susceptible to a

degradation phenomenon involving crack formation and propagation [49]. This happened in areas of devices where the stress level on the polymer is relatively high. Moreover, the residual polymer surface stress introduced during fabrication of the device can also cause the environmental stress cracking. In some biomedical devices, oxidative degradation can be a contributing mechanism. Implanted polyether-urethane devices that contain metallic components have been subject to bulk oxidation catalyzed by corrosion products of the metallic components [50, 51]. The enzymatic degradation is in the physiological environment is another PU degradation form. Even though the enzymes are designed for highly specific interactions with particular biological substrates, some appear capable of recognizing and acting upon 'unnatural' substrates including PUs [52]. It is found that enzymes are capable of altering polymer structure and there is a model for the biodegradation by hydrolytic enzymes attack [53].

Furthermore, all these degradation phenomena mentioned above are closely related to the surface re-organization of PUs. In PU-based materials, a microphase segregation process leads to the formation of a two-microphase structure with regions enriched in either hard or soft segments [54]. Due to the mobility of the soft segments in the PU, the segmented PUs on the surface varies in order to find the optimal hard/soft segment ratio that will be minimize the interfacial free energy. Commonly, there is a higher proportion of polar hard segment at the interface when the environment (water or blood) is polar and more non-polar soft segments at the surface when the environment is non-polar (air or vacuum). The change of the polymer chains conformation according to

the environmental polarity is important because the host response is largely determined by the surface composition of the material.

Action of degradation of PUs on inflammatory cells

During PU in-vivo degradation process, the white blood cell and the monocyte derived macrophage emerged as the predominant cell type that is surrounding the damage [55]. But it must be clearly stated that the macrophage takes its cue from the presence of the material and its unique chemistry. It is observed that the cellular composition of the inflammatory exudates surrounding the implanted material. The temporal variation in the acute inflammatory response, chronic inflammatory response, granulation tissue development and foreign body reaction to the implanted biomaterial was determined [56]. The foreign body reaction to a material in contact with tissue and/or blood cells proceeds according to the following time course. Neutrophil (PMN) appear within minutes along with monocytes, which then over the course of days differentiate into macrophage while adherent to the material. Eventually, the blood cells remaining adherent consist mainly of macrophage and foreign body giant cell, which may persist at the tissue-implant interface for the lifetime of the implant [57, 58].

The cellular interaction on the PUs may result in further biodegradation of PU whether it is desired or not. The general process of biodegradation has been studied on the environmental stress cracking of non-degradable PU many years ago, the mechanism is still not fully elucidated [50]. The release of oxidative and hydrolytic activities from the surrounding tissues, mainly including monocytes and giant cells, were involved in the

biodegradation process [59, 60]. For example, in some study, an environmental stress cracking was simulated in an in vitro accelerated biological model of oxidation using macrophage and $FeCl_2$. The action of the macrophage on the polymer surface cracking was inhibited by modifying the surface with a coated dexamethasone, which is an anti-inflammatory agent [61]. It is also found that polycarbonate PUs have less susceptible to oxidation than polyether-PUs [48, 62]. During degradation process, initially, neutrophils (PMN) are the primary source of reactive oxygen species releasing different amount of hypochlorous acid (HOCl), one of the most oxidative compounds, to the polymer surface where the macrophages were adhered [63]. Because of the oxidative potential of HOCl, PMN was involved in PU degradation as well even they do not remain at the site of implantation when the foreign body reaction becomes chronic. Various materials have different surfaces properties, the PMN can be activated differently on different surfaces and show the variety of in the release of superoxide anion, mac-1 expression and elastase [64, 65]. It was found that when superoxide dismutase modified PUs were implanted into rats, PMN-rich acute inflammatory infiltrates were reduced as well as the number of giant cells. However in another study, it was found that when PU, polyester-, polyether- or polycarbonate-based PU were treated with HOCl, significant inhibition of the subsequent hydrolysis by cholesterol esterase was observed [66, 67]. Phorbol myristate acetate (PMA), which stimulates the release of HOCl from PMN by the activation of protein kinase C, also inhibited radiolabel release elicited by PMN from PUs. Therefore, there is still lack in understanding the relationship between oxidative and hydrolytic enzyme processes during PU biodegradation.

There are also external forces and/or pathological processes that can influence the role of reactive oxygen species at implant sites; this may disturb the biodegradation pathway and the biocompatibility of the PUs in the application. As the implanted area is in the presence of some factors such as exposure to infectious agents or shear stress, PMN responses - the release of reactive oxygen species - were compromised in a distinct manner that is related to the material surface, which is know as foreign body associated infection [68]. This phenomenon often leads to infections and biofilm formation, which is notoriously resistant to antibiotics and creates the implanted device failure. Some studies showed that the macrophages surrounding PU implants released reactive oxygen species, which is PU surface dependant and caused tumor formation [69].

Chapter 3

RESEARCH OBJECTIVES

In our study, we proposed to synthesize a series of 'smart' polymers whose physical properties change in response to environmental stimuli, such as pH, ionic strength and temperature. This polymer was expected to be used for drug delivery, scaffold fabrication by novel ink-jet printing technology or other potential biomedical applications. Due to the chemical versatility and good elasticity, polyurethane was considered to be a good candidate for such a polymer. Therefore, we proposed to develop a series of novel degradable, elastic, anionic, and linear polyurethanes. The polyurethanes could be either synthesized from methylene di-*p*-phenyl-diisocyanate (MDI), polycaprolactone diol (PCL-diol) and N, N-*bis* (2-hydorxyethyl)-2-aminoethane-sulfonic acid (BES) chain extender, or from hexamethylene diisocyanate, polycaprolactone diol, and a bicine chain extender. In order to compare the chemical and physical properties with traditional polyurethanes, we used a polyurethane containing a 2,2-(methylimino) diethanol (MIDE) chain extender, which contains neutral methyl groups instead of ionic groups, as control; therefore, in comparison to the PUs with BES or bicine chain extender, the PU extended by MIDE has similar chemical structure but contains no ionic side groups. Because of the incorporation of negatively charged sulfonic acid or carboxyl acid side groups, the BES or bicine extended polymers were expected to have a better mechanical properties in dry condition, and better sensitivity to environmental stimuli than controls.

Specifically, for the BES chain extended polyurethane, we propose to investigate the blood compatibility by platelet attachment assay and pH-dependency for the scaffold fabrication by ink-jet printing technique. For the bicine chain extended polyurethane, we propose to investigate drug delivery and release properties from the solid scaffold. We will employ two model compounds for those studies, nile blue chloride and lysozyme build the relationship among environmental stimuli, swelling ratio and their release profile. We also propose to use the pH dependent properties of this novel polyurethane to fabricate scaffolds by drop-on-demand printing.

Part I: chapter 4

SYNTHESIS AND CHARACTERIZATION OF BIODEGRADABLE ELASTOMERIC POLYURETHANE SCAFFOLD FABRICATED BY THE INK-JET TECHNIQUE

Abstract

Biodegradable polyurethanes (PUs) were synthesized from methylene di-*p*-phenyldiisocyanate (MDI), polycaprolactone diol (PCL-diol) and N, N-*bis* (2-hydorxyethyl)-2-aminoethane-sulfonic acid (BES), serving as a hard segment, soft segment and chain extender respectively. MDI was chosen because it is widely used in reactivity and wide application in synthesis of biomedical polyurethanes due to its reactivity; PCL-diol was chosen because of its biodegradability; and BES was chosen because it allowed the introduction sulfonic acid groups onto the polymer chains. We evaluated the polyurethanes degradation rate, mechanical properties, hydrophilicity, antithrombogenecity, and ability to support fibroblast cell attachment and growth by comparing to polymers having a 2,2-(methylimino)diethanol (MIDE) chain extender. Mechanical testing demonstrated that the PUs containing BES have tensile strengths of about 17 MPa and elongations up to 400%, about three times the strength and four times the elongation than the MIDE based PUs. The polymers showed decreased in vitro degradation rates, lowers glass transition temperature (Tg) and hydrophilicity possibly due to enhanced micro-phase separation. Preliminary cytocompatibility studies showed that all the PUs are nontoxic, but PU containing BES exhibited much lower cell attachment and proliferation than the MIDE chain extended polymers. An in vitro platelet

adhesion assay showed lower platelet attachment on BES containing PU. Additionally, due to the existence of sulfonic acid groups, the BES extended PU became water-soluble in basic condition and insoluble in acidic condition, a phenomenon that is reversible at pH value of 8.7, making this a pH sensitive polymer attractive for bioprinting applications. By adding acetic acid into an inkjet cartridge and printing it onto a PU solution with pH above 8.7, precision fabricated scaffolds can be obtained, suggesting that BES based PUs are promising candidates as synthetic inks used for customizable fabrication of tissue engineering scaffolds.

1. Introduction

For decades, biomedical polyuretanes (PUs) have been intensively studied and used in various implant devices such as pacing leads insulation, catheters, intra-aortic balloons, cardiac valves and mammary implants [70, 71]. These polyurethane devices exhibited good biocompatibility and excellent mechanical properties; however, as most of these polyurethane devices are nondegradable, they may cause long-term foreign body reaction, may fail to integrate or exhibit material fatigue and are therefore not used as tissue engineering scaffolds [72]. Scaffolding materials have been selected from a plethora of biodegradable polymers, such as collagen, chitosan, hyaluronic acid (HA), poly(DL-lactide-co-glycolide) (PLGA), polylactic acid (PLLA), polyanhydride, polycarbonate, polyimide, polyamide, poly(amino acid), polyphosphazene, to name a few [73-75]. Although these polymers are well tolerated by cells *in vitro* and *in vivo*, the majorities are either too stiff with low flexibility or too soft with relatively low strength. To overcome those limitations, a number of degradable PUs have been introduced for a

range of biomedical applications varying from cardiovascular repair, cartilage implant, ligament regeneration, bone replacement to controlled drug/gene delivery [27, 76, 77].

It has been shown that incorporation of sulfonic groups into nondegradable PUs will improve the polymers' blood compatibility, an effect explained by principle that the electrostatic repulsion between the sulfonic groups and the blood proteins lessens protein adsorption and lowers platelet adhesion and activation [78, 79]. Several of these studies found that the incorporation of sulfonic groups also affected other physical properties, such as the glass transition, tensile strength, modulus, melt viscosity, relaxation behavior, and solution behavior. Generally, these polymers show a higher degree of water absorption than their non-sulfonated counterparts[79], and exhibit reduced mechanical properties in aqueous solutions due to their water absorption. Some researchers found that the increased sulfonic ion content in the PU backbone resulted in the water soluble polymers; other groups reported that the sulfonated PUs became water soluble in basic environment but water insoluble in acidic environment [80, 81]. However, there are no reports about how to utilize these pH sensitive polymers to fabricate scaffolds. Furthermore, although much research work has been done incorporating sulfonic groups into non-degradable PUs, there is, to our knowledge, no report about incorporating those groups into degradable PUs that may find applications in the tissue engineering arena.

Precision fabrication of biological scaffolds that provide support to the cells during growth and development into complex three-dimensional structures have recently gained attention. Because of the limitation of the traditional fabrication to control and predefine microstructure of the final scaffold, several techniques hitherto termed 'solid

freeform fabrication' (SFF), were recently adapted to custom fabricate scaffolds [82, 83]. These include stereo lithography [84], wax printers [85], and inkjet printing [86, 87]. The main advantages of these techniques are their capability to precisely control matrix architecture and their ability to be interfaced with computer imaging techniques, which make it possible to produce constructs with customized size and shape for tailor-specific tissue engineering applications [88]. Among them, the low-cost inkjet-printing technique was recently shown to possess particular advantages on generating three dimensional scaffold and cellular structures [89, 90]. The inkjet-printing technique allows simultaneous and precise controlled quantity of scaffolding materials , nutrients, therapeutic drugs, growth factors and other bioactive components to form cells/scaffold constructs for *in vitro* and *in vivo* growth [91].

Although inkjet-printing technique has advantages for biomedical scaffold fabrication, the viscosity requirements as well as the constraints of using only cell compatible and aqueous based inks limit the type of materials that could be used as scaffolds. The inks are required to be water soluble and easily solidifiable after printing to form scaffolds by either phase change or crosslinking due to environmental factors such as pH, ionic strength, electricity, magnetism, light intensity or enzymes. Moreover, those polymers need to be cell compatible and possess good mechanical properties. To date, most investigation on the inks used for precision scaffolds have been focused on very few natural polymers such as alginic acid, which is known to crosslink in calcium chloride solution through static force interaction among ions and polymer chains [92-94]. However, those natural polymers typically exhibit low mechanical properties or poor

functionality for specific applications. Therefore, the availability of cell compatible synthetic polymers used in printing process can form scaffolds with good mechanical properties will prove beneficial for tissue engineering applications.

In this study, a sulfonic acid containing polyurethane was synthesized from methylene di-*p*-phenyl-diisocyanate (MDI), polycaprolactone diol (PCL-diol) and N, N-*bis* (2-hydorxyethylhydroxyethyl)-2-aminoethane-sulfonic acid (BES) as the chain extender. The high mechanical properties was expected to be obtained by using MDI as hard segment, the degradability of the polyurethane by the incorporation of PCL-diol into soft segment, and the water solubility of polyurethane by the extra side groups of sulfonic acid in the chain exterder. The effects of sulfonic acid incorporation were evaluated by comparing with a non-sulfonic acid containing polyurethane, which had a 2,2-(methylimino) diethanol (MIDE)chain extender. MIDE was used because it has a similar chemical structure to BES but contains no sulfonic acid group as shown in Figure 1. Tecoflex®, a commercially available non-degradable biomedical-grade PU, was also used for comparison. Physiochemical property characterization methods, including attenuated total reflective-Fourier transform infrared spectroscopy (ATR-FTIR) was used to characterize the polymer structure, gel permeation chromatography (GPC) was conducted to measure the molecular weight of the polymers, differential scanning calorimetry (DSC) was applied to characterize the polymer thermal properties, water swelling rate analysis was used to measure the polymer hydrophilicity, tensile test was conducted to measure the mechanical properties, *in vitro* degradation rate analysis were performed to measure the degradability and scanning electron microscope (SEM)

analyses was performed to observe the porous scaffold structure. *In vitro* platelet adhesion assays were conducted for the preliminary investigation of the PUs' blood-contacting response. The cell viability and proliferation condition were evaluated by 3T3 fibroblasts culturing on both flat polymer membranes and fabricated scaffolds. Compared to the PU containing MIDE, PU containing BES was expected to exhibit higher mechanical properties, lower platelet attachment and water solubility in basic solution.

2. Materials and methods

2.1. Materials

Methylene di-p-phenyl-diisocyanate (MDI), N,N - Bis(2-hydroxyethyl) - 2 - aminoethanesulfonic acid (BES), 2,2-(methylimino) diethanol (MIDE), acetic acid, dichloromethane (CH_2Cl_2) and N,N-dimethylformamide (DMF) were obtained from Acros Organics Fine Chemicals (Geel, Belgium). Dimethyl sulfoxide (DMSO) was purchase from Fisher Scientific International. Stannous octoate ($Sn(oct)_2$, $Sn[CH_3(CH2)_3CH(C_2H_5)COO]_2$) and polycaprolactone diol with Mn=530 (PCL530) were purchased from Sigma-Aldrich (St. Louis, MO). MDI was purified by vacuum distillation. BES was vacuum dried at 60^{o}C for 48 hours before use. MIDE was distilled with calcium hydride (CaH_2) to eliminate moisture. DMSO was distilled over CaH_2 at atmospheric pressure under nitrogen protection. PCL530 was dehydrated in a vacuum oven at 60 ^{o}C for 48 h. $Sn(oct)_2$ was purified over 4A° molecular sieve with overnight stirring to eliminate trace water prior to use. Acetic acid, CH_2Cl_2 and DMF were used as

received. NIH 3T3 mouse fibroblasts (CRL-1658, ATCC, Manassas, VA) were used as a model cell type for cell viability and proliferation assay. Dulbecco's Modified Eagles Media (DMEM) augmented by 10% fetal bovine serum (FBS) and 1% antibiotics was used as culture media, all obtained from Sigma Chemical Company.

2.2. PU synthesis and membrane preparation

The polymers used in this study were synthesized by the traditional two-step method under nitrogen protection as described in Figure 1 [34]. Briefly, stoichiometry of the reaction was approximately 2:1:1 of dissocyanate (MDI): polyol (PCL530): chain extender (BES or MIDE). The MDI was dissolved in DMSO in a four-neck flask and PCL530/DMSO solution containing 1%wt $Sn(oct)_2$ as catalyst was added drop-wise at 60^oC. This mixture was allowed to react for 2.5 to 3 hours and then to cool down to room temperature. Following that, 5% w/v chain extender in DMSO was added drop-wise to the prepolymer solution under constant stirring for another 12 hours. After completion of the reaction, the polyurethane solution was precipitated into deionized water for at least 48 hours, washed thoroughly with ethanol for 6 hours at room temperature, and then dried in a vacuum oven at 60^oC for 48 hours before further use and characterization.

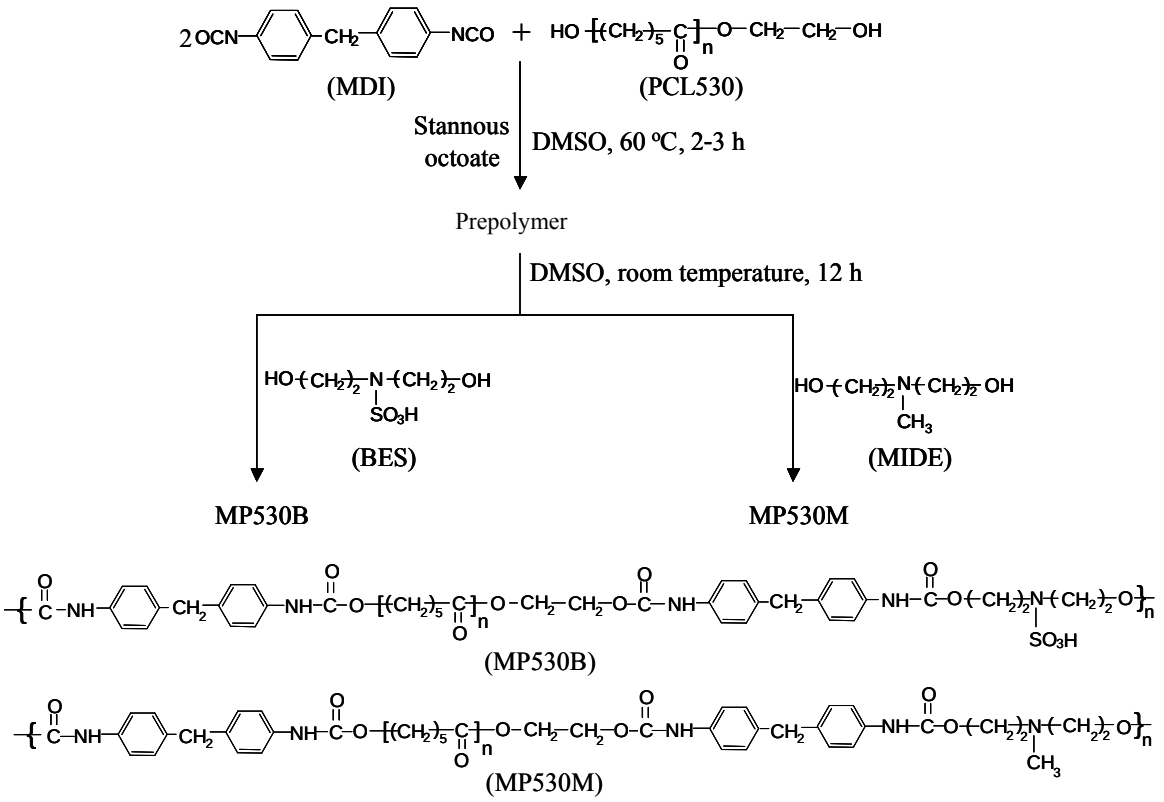

Figure 1: Synthesis scheme for the preparation of MDI, PCL530, MIDE or BES based PUs. Chain extender was changed to obtain materials with different functionalities.

The sample nomenclature and composition of all the polymers are designated with the first letter denoting the hard segment type (M=MDI), second letter and number denoting the soft segment and its molecular weight (P530=PCL diol with molecular weight 530), the final letter indicating the chain extender (B=BES and M=MIDE). As shown in Table 1, MP530B symbolizes the PU with molar ratio of 2:1:1 MDI, PCL with molecular weight 530 and BES as the chain extender; while MP530M symbolizes the PU with MIDE as the chain extender.

Table 1: Composition and properties of biodegradable PUs made from MDI, PCL530 and chain extender of BES or MIDE.

Materials	Composition	Mechanical Properties in Percentage to Tecoflex SG60				GPC	Swelling Ratio at 48 Hours
		Tensile Strength (%)		Elongation (%)		Mn	
	Molar Ratio	Dry	Wet	Dry	Wet	(g/mol)	(%)
MP530B	MDI/PCL/BES 2/1/1	63	11	55	109	162,000	4.7 ± 1.9
MP530M	MDI/PCL/MIDE 2/1/1	21	3	72	7	66,000	11.0 ± 0.9

Synthesized PU membranes were prepared by casting 8 % (W/V) DMF solution onto a Teflon mold and drying at 60 ^{o}C for 24 hours. Tecoflex® membranes were prepared by casting 8 % (W/V) CH_2Cl_2 solution onto a Teflon mold and drying at room temperature in a chemical hood for 4 hours, while covered by class plates to prevent formation of bubbles and surface defects. All the cast films were removed from the mold and further dried in a vacuum oven at 60 ^{o}C for 48 hours to remove residual solvent. The membranes had an average thickness of about 0.17 ± 0.03 mm and were stored in a desiccator at room temperature. The membranes were cut into appropriate size and used for mechanical test, water swelling rate analysis, *in-vitro* degradation assay and platelet adhesion experiment.

2.3. Bulk property characterization

The molecular weights of the synthesized polymers were determined by gel permeation chromatography (GPC; ThermoFisher Scientific, Waltham, MA). using polystyrene solutions in DMF (EasiCal PS-1, PolymerLabs, Amherst, MA) with molecular weights in a range of 580-7,500,000 Da as calibration standards.. The

polymers were dissolved at 0.25% (W/V) in the GPC carrier solvent and 20 μL samples were injected.

Attenuated total reflective-Fourier transform infrared spectroscopy (ATR-FTIR, Nicolet IR200) was used to characterize the chemical structure of synthesized PUs. Sixty-four scans at a resolution of 2 cm^{-1} were averaged. The samples for infrared analysis were prepared by solution casting of 8% (W/V) polymer in DMF directly onto KBr crystal plates and vacuum dried at 60^{o}C for 24 hours prior to characterization.

Thermal analysis was performed in Mettler Differential Scanning Calorimetry (DSC) analyzer (DSC 822e), with a heating rate of 20 °C/min under constant nitrogen flow. Polymer samples (70-90 mg) were heated to 50 °C for 10 min, quenched to -100 °C, maintained at this temperature for 10 min, then tested over the range from -50 to 180 °C at 20 °C/min.

Water absorption analysis was performed by measuring the swelling rate of the polymer membranes after immersion in deionized water at room temperature for 10 min, 25 min, 1 h, 1.5 h, 7 h and 48 h. The surface water on each sample was blotted with a filter paper before weighing. The swelling ratio was calculated by dividing the weight of the swollen sample by the weight of the dry sample. Three samples of each PU were measured to obtain the mean water swelling ratio and standard deviation.

For tensile tests, PU samples were cut from membranes into approximate 5.5×12 mm^2 rectangular strips. Tensile test were conducted using an Instron 4502 (Instron, Norwood, MA) at a crosshead speed of 25mm/min with maximum load of 10kN. Due to the application of polymers in water-rich environment such as culture media and live

tissues, measurements of the mechanical properties were carried out in both dry and wet conditions. Wet samples were prepared by saturating them in phosphate-buffered saline (PBS) for 12h at room temperature to reach the equilibrium. Three samples of each condition were measured to get an average tensile strength, elongation and standard deviation values.

2.4. *In-vitro* degradation assay

In vitro degradation of the PUs was evaluated by recording the samples weight loss, molecular weight changes, and mechanical properties changes over time in PBS buffer solution at 67 °C. Each PU sample cut from membrane was with the weight of about 14mg and the size of approximate 5.5 mm in width, 12 mm in length and 0.16 mm in thickness. The samples were placed in small vials separately filled with 1.5 ml PBS buffer solution containing 0.5% (W/V) sodium azide as antimicrobial agent. Those tubes were placed in a 67 °C water bath with gentle shake of approximate 70 - 80 RPM to simulate dynamic in vivo tissue environment. A higher temperature was used to accelerate the degradation rate. An established relationship with different temperatures is available to convert the degradation profile to 37 °C [76]. At each time point of week 1, 2, 3 and 4, 3 vials of each type of material were sampled, rinsed for 1 hour by deionized water and vacuum dried for three days before analysis of weight loss and molecular weight change. The PBS solution in each vial was collected for pH value measurement. After that, the PU stripes were then saturated by PBS buffer solution at room temperature for the tensile test in wet condition.

2.5. *In-vitro* cytocompatibility assay

PU solutions were evenly coated on 18mm diameter coverglass (n=6 for each time point and each material). After being dried at 60 °C in the oven for 12 h, samples were further dried in vacuum oven at 60 °C for 24 hours to eliminate the residual solvent. The samples were sterilized in 75% ethanol for 15 min, washed with sterile PBS three times, and then put into 12-well tissue culture plates. Fibroblasts cells were seeded at concentrations of 1.5×10^6 cells/ml on the polymer surfaces, after three hours, when cells were attached on the polymer surfaces, 2 ml media was added to each well to continue the culture for 9 days observation. Cell adhesion and proliferation on the sample surfaces were examined at 3, 5, 7, and 9 days by phase contrast microscopy and total cell populations; culture dishes and Tecoflex® coated cover glasses were used as negative controls.

2.6. Platelet adhesion characterization

Fresh pig blood was obtained from a local slaughter house, collected into 8.5 ml venous blood collection tubes (Vacutainer®, BD Company) that are pre-filled with1.5ml anticoagulant containing 0.22% trisodium citrate, 0.08% citric acid and 0.24% dextrose. Platelet-rich plasma (PRP) was obtained from the blood by centrifugation at 750 g for 10 min; the upper layer was collected and added to an equal volume of PBS. The platelet concentration of PRP was measured by Coulter counter (Z2 COULTER COUNTER®, Beckman Coulter, Inc.) and adjusted to be about 5.2×10^7 platelets/ml by dilution.

Polyurethane membranes were punched into round shaped films with diameter in 8 mm (n=6 for each sample) and equilibrated in PBS at 37 °C overnight. After removing the samples from the PBS solution, the samples were immersed in PRP and incubated in a cell culture incubator at 37 °C and 5% CO_2 atmosphere for 1 h. Following incubation, the samples were gently rinsed with PBS solution three times to wash away any nonattached platelets, moved to a new 12-well plate; 400 µl of 1% Triton-X100 solution was added into each well, and incubated at 37 °C for 1h to lyse the adherent platelets. Lactate dehydrogenase (LDH) activity was measured using a CytoTox 96® Non-Radioactive Assay kit (Promega Corp.). Briefly, the stable LDH released from lysed platelets was coupled to a tetrazolium salt (2-p-iodophenyl-3-p-nitrophenyl-5-phenyl tetrazolium chloride, INT) and caused the conversion of INT into a red formzan product. The concentration of red product was indirectly obtained by measuring the light absorbance at 490 nm, and the value of light absorbance was proportional to the number of platelets. Tecoflex® was used as control. Six samples of each PU were measured to obtain the mean light absorbance value and standard deviation.

2.7. PU neutralization and scaffold fabrication

PU neutralization was carried out by first dissolving MP530B in DMF to form a 12% (W/V) solution. A calculated stoichiometric amount of 1 mol/L sodium hydroxide water solution was added and reacted at room temperature for 1 h as described in Figure 7C, sulfonic acid groups on chain extender were reacted to sulfonic ions and the neutralized polymer became water soluble. The neutralized polymer/DMF solution was

further diluted by deionized water to 2.5% (W/V) for scaffold fabrication. The HP desktop 3900 printer and HP 21 black ink cartridge was modified to fabricate single-layer patterns as described elsewhere [95]. The 50% (V/V) acetic acid (HAc) water solution was filled into the cartridge. The 2% (W/V) polymer solution was dropped on the glass slides to form an even liquid layer on the standard glass slide surface, this glass slides was then placed onto the print stage mounted under the print heads. The patterns that consisted of letters (CLEMSON, font: Times and New Roman, size 16) or rowed rings were designated using Microsoft Words to program the printer. The HAc solution was printed out in one cartridge pass to the glass slide and reacted with the polymer solution (Figure 7C), thus the final expected patters on the glass slide were obtained. These scaffolds on the glass slides were dehydrated by immersion in a series of ethanol/water solution (50, 70, 85, 90, 100% V/V) before critical point drying with liquid CO_2 as transitional liquid medium. After sputter coating with gold, samples were observed by (Hitachi s7400) scanning electron microscope (SEM 3500, Hitachi Ltd) at magnifications of 400, 2.5k and 20k.

2.8. Fibroblast seeding on printed scaffold

Dehydrated scaffolds were sterilized with 75% ethanol for 24 hours and vacuum dried for another 24 hours. Before cell seeding, scaffolds were rehydrated in sterilized 0.1 M PBS for one hour.

Fibroblasts cells were seeded at concentrations of 1.5×10^8 cells/ml on the printed O-ring shaped polymer scaffold on the slide in petrish (100mm*20mm), after three hours,

when cells were attached on the polymer, 10 ml media was added to into the petridish to fully cover the scaffold, this petridish was allowed to continue the culture for 5 days observation. At day 5, the slide with scaffold was transferred to a clean petridish, 10ml prepared calcein AM (Molecular Probes, Eugene) PBS solution (5 ul/10 ml) was added onto scaffold to stain the cells for 45 minutes in incubator. The sample was then examined by UV light fluorescence microscopy (Nikon Diaphot 300) to check the cell morphology on printed scaffold.

3. Results and discussion

3.1. Infrared spectroscopy

The FTIR absorption spectra of the PUs at room temperature are shown in Figure 2. MP530B and MP530M having same stoichiometric ratio of initial reactants as shown in Table 1, exhibited similar spectra between 400 – 4000 cm^{-1}. However, an extra absorbance peak at approximate 1043 cm^{-1} was observed in MP530B spectra, which corresponds to the -SO_3- symmetric stretching absorbance [96, 97] and indicates the successful synthesis of sulfonic acid incorporated PU.

In PUs, hydrogen bonding can occur between the urethane groups, hard segment carbonyl oxygen and soft segment carbonyl oxygen. In PU anionomers hydrogen bonding can also occur with a proton accepting ionic group. The ratio of the hydrogen bonded carbonyl absorbance of C=O stretching vibration at about 1704 cm^{-1} to the free carbonyl absorbance at about 1731 cm^{-1} provide a qualitative estimation of hydrogen bonds and phase separation in PUs [98]. As shown in Figure 2, both MP530B and MP530M show

the hydrogen bonded and free carbonyl stretching vibration absorption bands at 1704 cm^{-1} and 1731 cm^{-1}, the ratio of bonded carbonyl to free carbonyl of MP530B is about 0.87 and the ratio of MP530M is about 0.95 respectively. The lower ratio of MP530B than MP530M corresponds to the higher content of free carbonyl in MP530B than that in MP530M, indicating the formation of the hydrogen bonds between the pendant sulfonic acid groups and urethane groups. These hydrogen bonds further disrupt the hard segment hydrogen bonding and packing among carbonyl and urethanes groups, the change in hard-segment packing thus enhances the micro-phase separation in the MP530B. The higher phase separation properties of MP530B can result in the physical properties change such as lower glass transition temperature, higher mechanical properties compared to the control, the phase separation properties will be further discussed in subsequent thermal properties characterization.

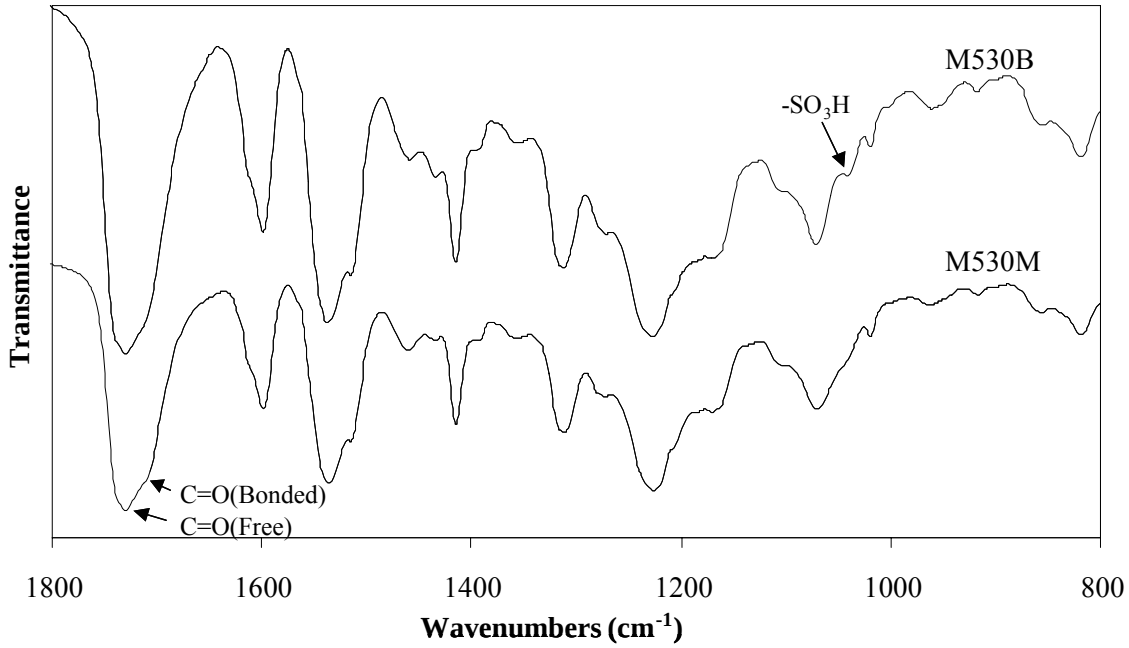

Figure 2: FTIR spectra of the PUs with different chain extenders. The band at 1042 cm^{-1} corresponds to the symmetric stretching mode of -SO_3-, the band at 1704 cm^{-1} and 1731 cm^{-1} correspond to the stretching mode of the hydrogen bonded and free carbonyl group respectively. The ratio of bonded carbonyl absorbance to free carbonyl absorbance of

3.2. Thermal transition

The differential scanning calorimetry (DSC) results for two types of PUs are shown in Figure 3. Glass transition temperatures (Tgs) of 8 °C and 19 °C were observed for MP530B and MP530M respectively. Both Tgs are lower than 37 °C, indicating that two types of PUs can maintain elasticity at body temperature. These Tg values are also substantially higher than that of pure PCL (Tg = -58 °C), indicating phase mixing of hard segments and soft segments in the PCL based PUs [99, 100]. The lower Tg value of MP530B than MP530B suggests that the BES chain extended PU has higher phase separation degree than its MIDE chain extended analog, which is consistent with the results from FTIR observation. The enhanced phase separation in MP530B can be explained by the significantly high polarity difference between the sulfonic acid containing hard segment and soft segment. It has been intensely studied that the typical character of phase separation in all PUs is attributed to the polarity difference of polar hard segment and un-polar soft segment, the higher incompatibility of the hard segment and soft segment results in the higher phase separation. In our study, the PCL in polymer soft segment can be considered to be of very low polarity, the sulfonic acid in the chain extender of MP530B has much higher polarity than methyl group of MIDE in MP530M, therefore, the higher polarity difference of hard segment and soft segment resulted in the higher phase separation in MP530B.

The change in the heating capacity (ΔCp) at Tg is associated with the mobility of the PU chains that are in a rubbery state below Tg [99]. The investigation of ΔCp can

further reveal the microphase separation in PUs, and the lower ΔCp indicates the higher phase separation. As shown in Figure 3, ΔCp is 0.48 J/(g °C) for MP530B and 0.52 J/(g °C) for MP530M respectively, a value that may be significant when taken together with the Tg shifts. The chain extenders in MP530B and MP530M have similar structure - the tertiary nitrogen atoms in chain extenders can induce the free rotation of the polymer chains, and the pendent groups on nitrogen atoms may further enhance the phase separation [42]. However, due to the significant polarity difference between the pendant sulfonic acid group in BES and methyl group in MIDE, the final chain extended PUs exhibit different thermal properties. In the BES extended PU, the pendent groups of sulfonic acids in BES have much higher polarity than the methyl pendent groups in the MIDE extended PU, resulting in much higher ionic interactions among polymer chains and strong physical crosslinks. From this analysis we conclude that the effect of sulfonic acid outweighs the effect of the tertiary nitrogen atoms. Therefore, with extra polar sulfonic acid in the chain extender, MP530B exhibited the enhanced hard-segment domain cohesion and decreased chains mobility in rubbery state in comparison with MP530M.

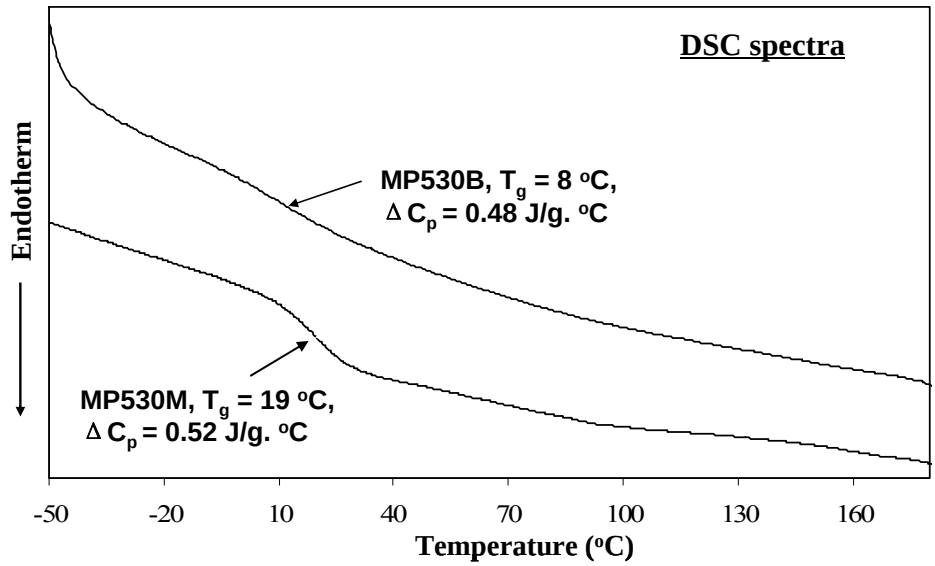

Figure 3: DSC thermograms of two types of biodegradable PUs of MP530B and MP530M. The curve on the top shows the thermal behavior of MP530B with Tg at 8 °C and ΔCp of 0.48 J/g °C. The curve on the bottom shows the thermal behavior of MP530M with Tg at 19 °C and ΔCp of 0.52 J/g °C.

3.3. Water absorption

Water absorption analysis was performed by measurement of swelling rate of PUs after immersion in deionized water at room temperature. The 7-hour kinetic water absorption profiles in Figure 4 show that, as expected, the amount of water in PUs initially increases rapidly, and then gradually reaches the plateau after 7 hours. A swelling equilibrium is reached after 48 hours in water; the final values of swelling rate are documented in Table . In this study, MP530B exhibited much lower water absorption rate and lower equilibrium swelling rate than that of MP530M, which is mainly attributed to the highly phase separation of BES chain extended polymers. Although the nitrogen atoms and pendent sulfonic acid groups in MP530B have certain degree of hydrophilicity, the high degree of phase separation limits the polymer chains mobility, thus limits the formation of hydrogen bonds between water and polymer chains. Water absorption in

MP530B took longer to reach the plateau value Figure 4, which reflects the lower mobility of the polymer chains and limited ability of polymer chains to combine. Compared to MP530B, MP530M exhibited higher water absorption rates and higher final swelling rates, which can be explained by the lower polarity of chain extender MIDE and the presence of nitrogen atoms. The polymer chains of MP530M have higher phase mixing and polymer chains mobility, which further resulted in the higher possibility of the hydrogen bonds formation among water molecules and polymer chains. As also seen in the figure, the shorter time for MP530M to reach the plateau value also reflects the higher polymer chains mobility and higher microphase mixing. Therefore, the degree of microphase separation in both PUs appears to be the primary driving force determining the PU's water absorption properties.

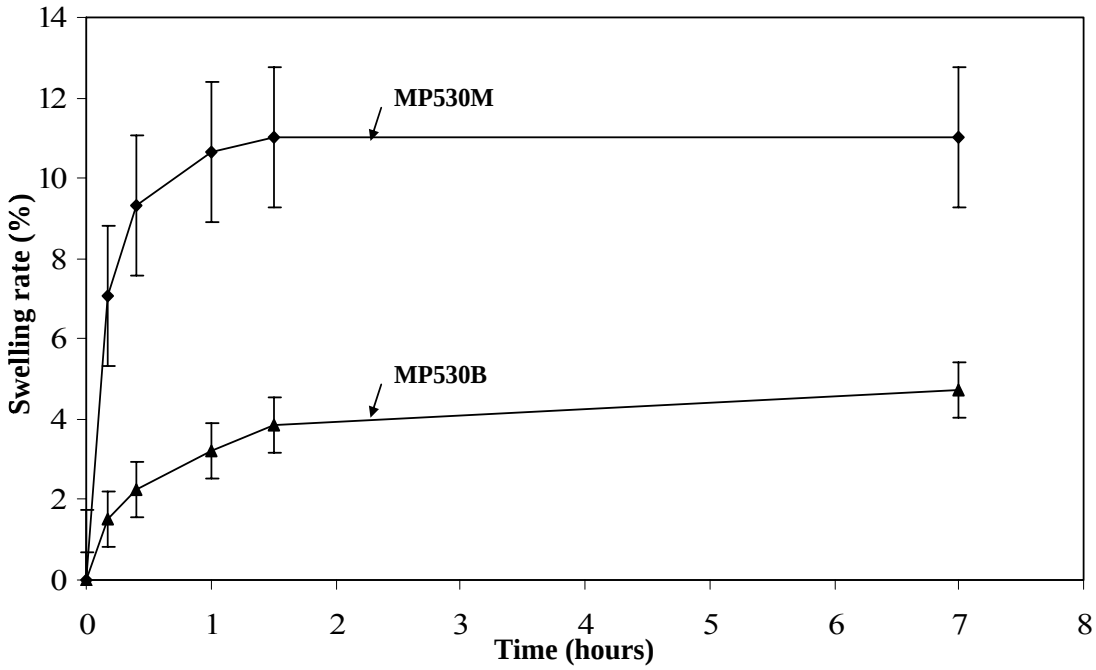

Figure 4: Swelling rate of two types of PU samples in water at room temperature. MP530B exhibited much lower swelling rate than MP530M in 7 h assay.

3.4. Mechanical properties

The elastomeric properties of the polyurethane are derived from the phase separation of the hard and soft segments, this phase separation occurs because of the incompatibility of the mainly non-polar soft segment with the polar hard segment. The stiff and immobile urethane hard segment domains serve as cross-links between the uncoiled and flexible soft segment domains. Upon mechanical deformation the hard segment become aligned while soft segment become uncoiled, which bring about the high tensile strength, elongation to the polyurethanes [34]. In this study, the mechanical properties of MP530B, MP530M are reported in Table 1 as a percentage of the Tecoflex control which has a reported ultimate tensile strength of 41 MPa and 400% elongation at break. MP530B exhibits three times the tensile strength of MP530M in dry conditions and approximately 2/3 that of Tecoflex. When saturated with PBS, the ultimate tensile strength of MP530B decreases to approximately 10% of the Tecoflex strength (~4 MPa); MP530M decreases to approximately 3% of the Tecoflex strength. The higher mechanical properties of MP530B can be explained by two reasons, first, the incorporation of the polar sulfonic acid in the polymer chains formed ion aggregates, increased hard segment polarity and served as extra physical crosslinks in the polymer, thereby increasing microphase separation and reinforcing the polymer chains interaction; second, the lower molecular weight of MP530M, which is about 40% of the Mn of MP530B, decreased the polymer chains integrity and interaction.

As shown in Table 1, elongation at break of MP530B was about half that of

Texoflex and about the same when saturated with PBS. These changes are attributed to the interaction between the sulfonic groups and water molecules through hydrogen bonding, which outcompete the polymer-polymer hydrogen bonds, thereby weakening the material. On the other hand, water can also increase the polymer elongation by serving as inter-chains 'lubricant' or 'plasticizer' in the polymer matrix [101], which was in favor of the long polymer chains realignment at high deformation, thereby enhanced the polymer matrix integrity in wet condition. MP530M exhibited both decreases of tensile strength and elongation in wet condition, Due to the low molecular weight and short polymer chain length of MP530M used in this study, a high percentage of polymer-polymer hydrogen bonds were replaced by water-polymer hydrogen bonds, and as a result, the polymer chains interaction was seriously interrupted, resulting in decreased elongation.

Mechanical properties of the control MP530M have been reported previously [42]. However, that study did not compare the properties to a known control. As absolute values for tensile strength vary considerably depending on specimen's size, preparation and testing parameters such as pulling speed, we chose here to compare the polymers to Tecoflex as it has been well characterized A direct comparison between MP530B and MP530M of the previous study is hence not possible. The high elasticity and tensile strength of MP530B is essential for engineering tissues with high elasticity, such as muscle, tendon, ligament, cardiovascular and vocal cord. In this study, although the tensile strength of MP530B in wet condition is lower than that of Tecoflex, the strength is still sufficient for most tissue engineering applications [102].

3.5. *In vitro* degradation assay

Because two types of PUs contain the soft segment of MDI, PCL and MIDE or BES, the *In vitro* degradation process is considered to be hydrolysis of the water sensitive groups such as ester and urethane groups. The hydrolysis procedure for the PUs includes three steps: at first step, water molecules enter the polymer bulk and attack ester and urethane groups, the long polymer chains were broken into short polymer chains, acidic substances were released and hydrolysis procedure is self accelerated in bulk at low pH micro-environment, the PU molecular weight accordingly decreases but the mass loss lags behind it because those degraded polymer chains are still water insoluble; in the second step, the short polymer chains are further hydrolyzed into small water soluble molecules, which results in a PU molecular weight drop, pH decrease and obvious mass loss. In this study, the degradation behavior of MP530B and MP530M were examined by measuring the molecular weight, mass loss, tensile strength and pH value. To speed up the degradation procedure to a measurable range, environmental temperature of 67 °C was employed. It has been reported that the degradation rate of MDI and PCL based PUs at 37 °C is about 1/20 of the degradation rate at 77 °C [76]; thereby, the degradation rate of MP530B and MP530M at 37 °C will be approximate 1/9 of the degradation rate at 67 °C according to Arrhenius' equation and assuming similar activation energies and pre-exponential factors. However, the rates should be taken as a guide and will need to be verified by in vivo experiments. As seen from Figure 5, MP530B exhibited much lower mass loss and molecular weight loss than MP530M. The molecular weight of

MP530B decreased by 20% at week 3 and that of MP530M decreased by 70% at week 2; the pH value of degradation solution of MP530B decreased from 7.4 to 7.09 ± 0.02 and that of MP530M decreased from 7.4 to 7.30 ± 0.02 after four weeks. The degradation rate of MP530M was about 4 – 10 times faster than that of MP530B. This result can be explained by the degree of microphase separation and initial molecular weight of polymers. The high phase mixing of MP530M caused the more flexibility of polymer chain, the low initial molecular weight of MP530M also resulted in the lower polymer chains interaction; both facilitating easy attack of water molecules to the backbone, which further increased the rate of hydrolysis. Although MP530B has the sulfonic acid groups that are hydrophilic, the high microphase separation can increase the polymer chains interaction and resist the attack of water molecules to ester groups, hence slow down the hydrolysis procedure. Interestingly, because MP530B released sulfonic acid groups from chain extender and caproic acid from soft segment, while MP530M only release caproic acid during hydrolysis, the MP530B degradation solution was more acidic than that of MP530M degradation solution. Considering this, the lower pH environment was expected to accelerate the hydrolysis procedure. However, in comparison of MP530M, the more acidic MP530B exhibited lower degradation rate in the assay. Thus, we may conclude that during MP530B degradation, the microphase separation played a dominant role over the self-catalysis by acidic environment. On the other hand, compared to the pH value change from 7.4 to 3.9 during polylactide acid (PLA) degradation at 77 °C in 4 days [42], the degradation products of MP530B and MP530M are not expected to significantly influence pH in the culture media *in vitro* at 37 °C.

The tensile strength as a function of *in vitro* degradation time is shown in Figure 5C. MP530B lost only about 15% tensile strength after 4 weeks while MP530M lost about 85% compared to a 38% and 85% loss of molecular weight respectively. Obviously, the influence of water on the tensile strength change of MP530B during degradation is much weaker than that on MP530M. Moreover, MP530B showed the lower tensile strength loss than molecular weight loss, indicating that the higher micro-phase separation and ionic force still maintained the polymer's integration. The property that MP530B can maintain the mechanical properties during degradation may be an advantage for the tissue engineering application of MP530B as long-term degrading scaffolds.

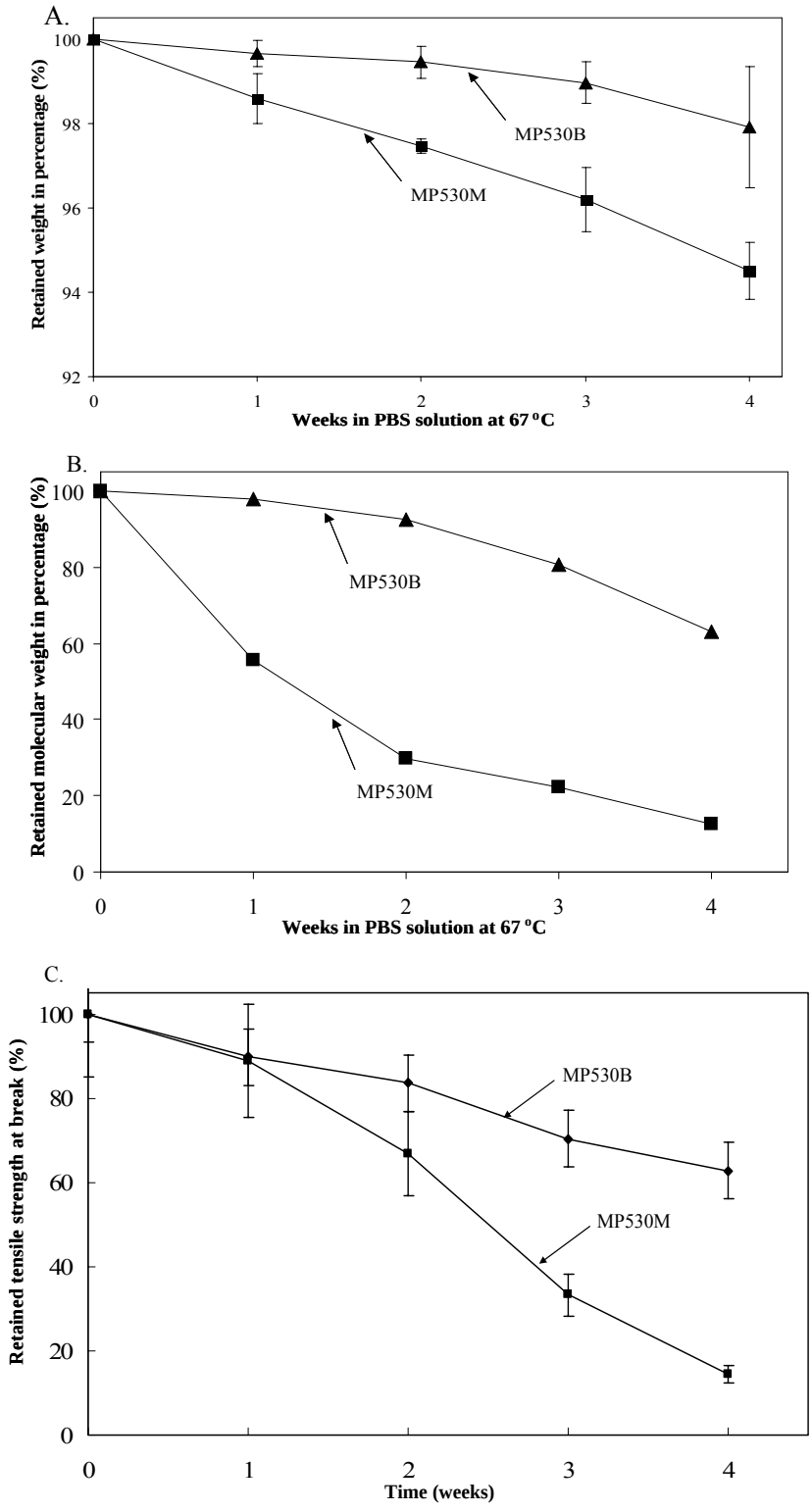

Figure 5: Degradation behavior of two types of PUs in PBS solution at 67 °C: (A) The average retained weight of MP530B and MP530M change as a function of weeks in PBS. (B) The average retained molecular weight of MP530B and MP530M change as a function of weeks in PBS. (C) The change of tensile strength of MP530B and MP530M as a function of weeks in PBS.

3.6. Cytocompatibility

The difference of cell proliferation rates on different material can be attributed to the cell-material interactions. Some recent studies have compared effects of surface charges on cell adhesion. Some demonstrated greater cell attachment and spreading on hydrophilic, positively charged glass surfaces versus hydrophobic surfaces [103]. Other work has demonstrated greater cell attachment and spreading on negatively charged and hydrophilic glass surface relative to hydrophilic glass surfaces[104]; yet other work demonstrated lower cell attachment and normal cell spreading on negatively charged glass surface [105]. Looking specifically at sulfonation, increased cell attachment and proliferation was documented with increases surface sulfonation density of polystyrene/poly(methyl methacrylate) copolymers [106]. To examine the cytocompatibility of the PUs in this study, fibroblasts were seeded on the membrane samples of MP530B, MP530M, Tecoflex and tissue culture dishes. Tecoflex and non-coated petridishes were used as control. As shown in Figure 6B, fibroblasts were attaching and proliferating on all the samples with varying densities with normal flattened appearance, indicating the existence of the different cell-material interactions for each material but all of them were cytocompatible. Fibroblasts proliferated fastest on MP530M and petridish controls; there were no statistical differences in cell numbers for cell populations grown on MP530M and culture dishes. Proliferation of fibroblasts on both MP530B and the Tecoflex controls were significantly lower than that of MP530M or culture dishes; no statistical difference was found between cell proliferation rates on the MP530B and Tecoflex. As qualitatively shown in Figure 6A, the low cell proliferation

rate of fibroblasts on MP530B is most likely attributed to the existence of negative sulfonic acid groups. In cell culture, the sulfonic acid on the materials surface can be ionized by culture media (pH = 7.4), and because the flexibility of the polymer chains, the ionized sulfonic groups can form a thin negatively charged layer on the substrate surface. This layer may repel the fibroblast attachment by the electrostatic interaction. Protein adsorption on these charged polymers may also be low, but has not been investigated in this study. The similar reason may also be used to explain the low cell proliferation on Tecoflex controls, which is made from MDI, poly(tetramethylene oxide) (PTMO) and butane diol (BD). The soft segment PTMO in Tecoflex contains sufficient amount of oxygen atoms that provide rich negative electrons, the electron-rich soft segment can accumulate on the substrate surface due to the polymer chains flexibility, thus form the similar electrostatic interaction as that of MP530B. As a comparison, MP530M exhibit good cell proliferation rate during 9 days culture, this can also be explained by cell-material electrostatic interaction, chain flexibility and hydrophilicity. In MP530M, the tertiary nitrogen atoms in chain extender MIDE can form cationic groups in the water and give a slightly positive polarity on the polymer chains. In culture media the polymer chains can change the conformation to form a positively charged layer on the substrate, which will interact with negatively charged cell membrane surface and most serum proteins, thus promote cell attachment and proliferation.

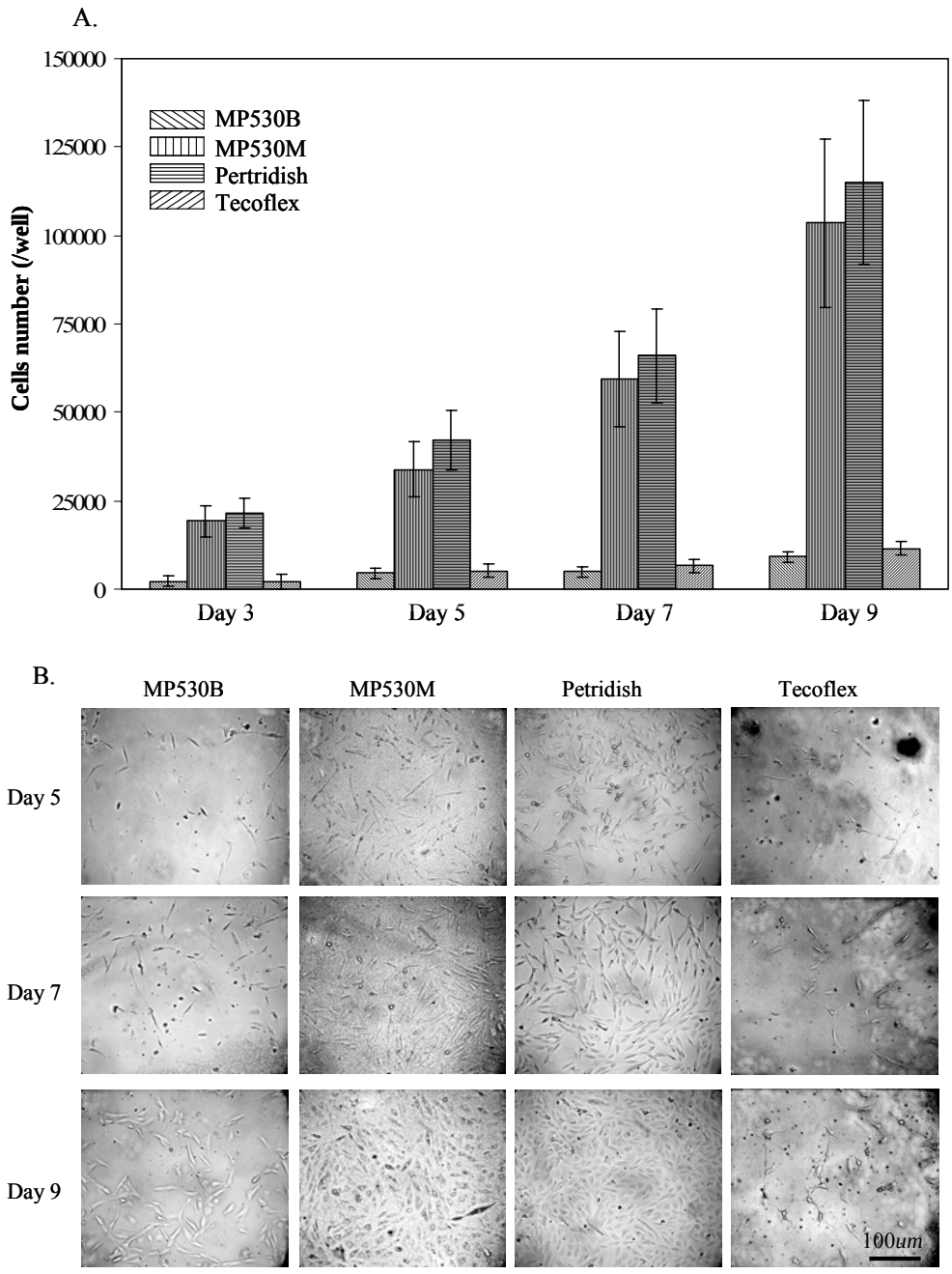

Figure 6: Cytocompatiblity assay for the MP530B and MP530M membranes. Petridish and Tecoflex membranes were employed as control: (A) quantitative assays of cell attachment and proliferation on MP530B, MP530M, petridish control and Tecoflex control. Data represent the mean of three samples ($P<0.05$). (B) Phase contrast micrographs of NIH 3T3 fibroblasts grown on the monolayer of each type of polymers at three time points. Cells on four types of polymer membranes exhibited spread patterns at each time point, while MP530M and petridish exhibited higher cell attachment and proliferation than that of MP530B and Tecoflex.

3.7. Platelet adhesion

Blood compatibility of a biomaterial can be reflected by the ability to prevent or reduce the formation of thromboemboli in cardiovascular environment. A simplified procedure of thrombus formation on biomaterials includes enzyme activation, protein absorbance, platelet adhesion, activation and shape change, generation of thrombus etc [107]. Therefore, a platelet adhesion study was conducted to investigate one aspect of the material's blood compatibility. In this study, Platelet adhesion on MP530B, MP530M and Tecoflex were quantified by measuring the amount of LDH released from the lysed platelets that adhered on the surface of each material. In platelet attachment study, the LDH assay for the Tecoflex and MP530B exhibited similar UV (490 nm) absorbance (0.013±0.002 and 0.014±0.004 respectively) and the LDH assay for the MP530M exhibited significantly higher UV absorbance (0.028±0.007), there was no statistical difference between the sample of MP530B and Tecoflex. These results indicate that MP530B and Tecoflex show much lower platelet adhesion than that of MP530M. Tecoflex has been used as a cardiovascular biomaterial for decades, and we rationalize that due to the similarity in the elasticity and anti platelet adhesion property of Tecoflex and MP530B, MP530B may find potential applications in cardiovascular tissue engineering.

PUs have been used in cardiovascular area for many years, and the good blood compatibility have been explained by different factors such as phase separated morphology [108], hydrophilicity [109], ionic charges and surface composition [110, 111]. In this study, both MP530B and Tecoflex exhibited low platelet adhesion. However,

considering the different chemical composition, different factors may be responsible for improving the material's blood compatibility. The low platelet adhesion on MP530B may be explained by the electrostatic interaction between polymer and platelet interface. In the culture media, the ionized sulfonic group accumulated on the polymer-media surface through the chain rotation, and this negative charged polymer surface can prohibit the approach of the negatively charged platelet membrane. So the ionic groups might have played a decisive role in platelet adhesion for MP530B, similar to the cell proliferation on MP530B. While the low platelet adhesion on Tecoflex may be attributed to the higher surface PTMO soft segments concentration [111], and the high content oxygen atoms in the soft segment, which provide large amount of electrons, can also partially contribute to the low platelet adhesion. In LDH assay, MP530M shows higher platelet adhesion than both MP530B and Tecoflex. Considering the positively charged tertiary nitrogen groups of MP530M at the pH of the media, platelets attachment may be facilitated by electrostatic interaction. However, the platelet adhesion on the materials is a complicated procedure including instant protein adsorption on the materials, protein deformation and protein reaction to the blood, and therefore protein adsorption is thought to regulate all the subsequent blood-material interactions [111].Protein adsorption experiments will be carried out in another study to further reveal the blood compatibility of MP530B.

3.8. Scaffold fabrication by ink jet printing technology and cell culture on the scaffold

To build scaffolds by ink-jet printing technique, a HP inkjet printer was modified as described previously [88]. The standard glass slides in the chamber of the printer were

evenly coated with a 2.5% (W/V) ionized PU solution. The ink cartridge was filled with 50% (V/V) HAc solution, which can be printed onto selected areas of the PU solution according to a pre-designed pattern Upon impact of the droplets the hydrogen ions in HAc solution reacted with pendent sulfonic ions on the polymer chains according to the chemical reaction shown in Figure 7C, causing the polymer to precipitate. This reaction is reversible, as the pattern was observed be gradually re-ionized and dissolved into water at pH higher than 8.7. However, at physiological pH the patterns remain solid. As shown in Figure 7, different letters (CLEMSON) and rings could be printed on identically computer-designed patterns, indicating that the MP530B can be easily used for the fabrication of the scaffold. Furthermore, MP530B can also be adapted to fabricate three dimensional patterns using the method described earlier [88], the related work is carried on in our lab.

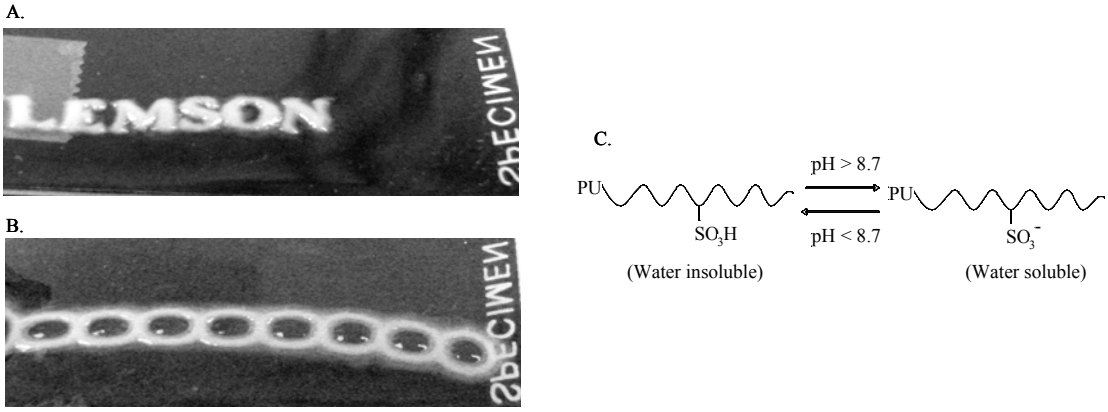

Figure 7: Photograph of the patterns printed on glass slides by inkjet printing technique. 50% (V/V) acetic acid water solution in HP 21 cartridge was printed out by one pass on MP530B solution coated glass slide. Patterns immediately formed in 1 second after printing. (A) Separate letters printed on the stand glass slides; (B) Contacted O-rings printed on the standard glass slides. All the patterns were computer designed by Microsoft Office software. The letters fixed on the right side of the standard glass slides were used as size control; (C) Schematic diagram shows that MP530B in the solution was neutralized and became soluble with pH higher than 8.7, this reaction is revisable with solution pH value adjusted lower than 8.7. This reaction was utilized for the scaffold fabrication by ink-jet printer.

Figure 8 shows the microstructure of the printed patterns by SEM observation. The patterns exhibited porous three-dimensional morphology. The primary structure at low magnification showed the number of pores with size between 10 to 30 μm, which could allow cell penetration. On the inner wall of those large size pores, the secondary structure at high magnification showed numerous pores with average size less than 100 nm evenly distributed and interconnected. This interconnection represents a great advantage for cell growth in the scaffold as it would be able to help the nutrients and growth factors transportation, gas penetration, signal transmission among cells distributed in the large size pores. The formation of this particular primary and secondary porous scaffold can be explained by surface gelling mechanism [88], in which the surface of the HAc droplets immediately reacted with PU solution, forming a capsule or the first shell around the droplets, thus the big size pores formed at this step. Due to the high concentration of HAc in the capsules and the separation of surrounding shell, the HAc gradually diffuse to the outside to react with PU solution. During this diffusion, the concentration of HAc decreased with the penetration into polymer solution, and the PU solution in the periphery of the droplets was then reacted with HAc into solid PU. The diffusion of the HAc through the first shell then resulted in the second shell. As this shell formation and ion diffusion continues, porous and layered structures of shells are formed. It has been reported that size of ink droplet can be influenced during scaffold printing by cartridge orifice size, cartridge-substrate working distance, ink properties, printer controlling parameters and so on [86, 88, 90, 112]. Therefore, as one of convenient adjusting methods, the large pore size in the primary structure of the scaffold can be

adjusted by changing the cartridge with different orifice size; while the small pore size in the secondary structure can be adjust by changing the HAc and/or polymer solution concentration. Our lab is studying the relationship among those factors to obtain more functional scaffolds.

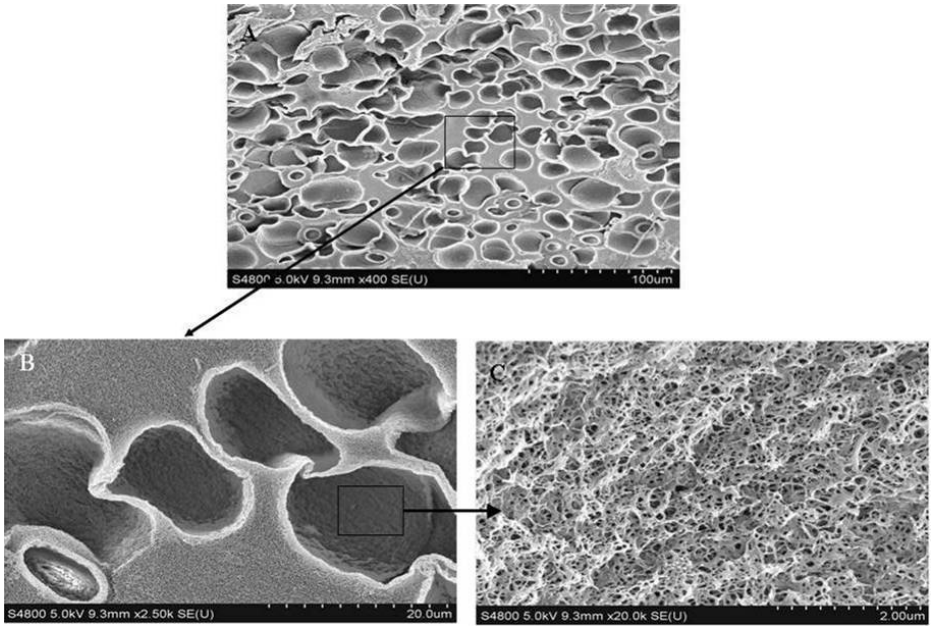

Figure 8: SEM images of the PU scaffold showing, (A)(B) Primary structures at different magnifications show the porous structure with pore size ranging from 10 to 30 μm. (C) Secondary structure shows the porous structure with uniform and inter-connective pores, the average size of pores is less than 1 μm. (A) Magnification 400x, (B) Magnification 2500x, (C) Magnification 20,000x.

Figure 9 shows the microstructure of the printed O-ring patterns by optical microscopic examination after 5 days fibroblast culture. Compared to the SEM observation at high magnification, at 10x magnification a number of pores with size between 10 to 150 μm can be observed, this higher average pore size may be caused by the hydration of the scaffold during cell culture and uneven distribution of the pores.

After 5 days culture, fibroblasts were found to attach and proliferate on the porous scaffold, and a number of the cells penetrated into the pores with size 20 μm or higher.

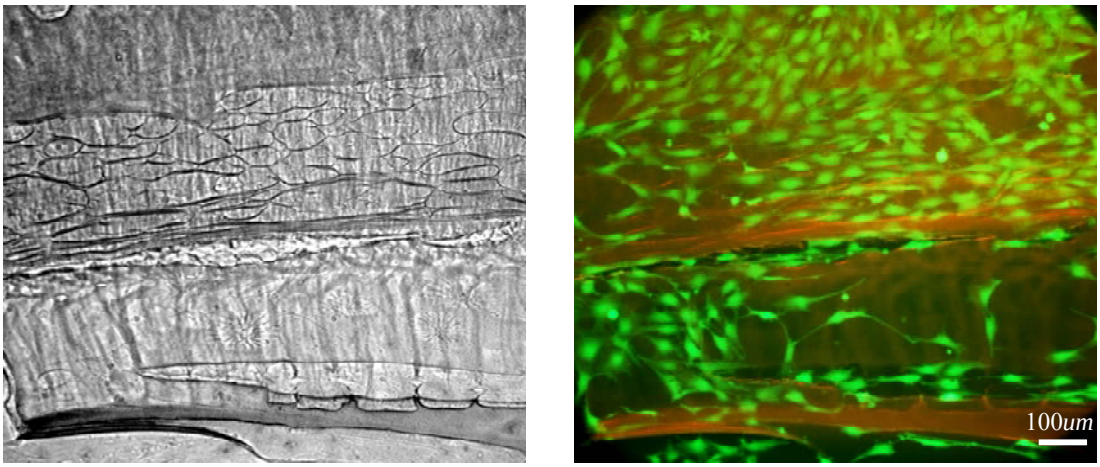

(A) (B)

Figure 9: Microscopic examination of the fibroblast proliferation on the printed O-ring scaffold after 5 days culture, (A) Micrograph of the hydrated O-ring scaffold by phase contrast microscopy, the picture exhibited the porous structure. The pore size observed by optical microscopy was between 10 μm and 150 μm; (B) Fluorescent micrograph of the fibroblast proliferation on the porous O-ring scaffold. Cells were stained in green by calcein AM, and the red area indicated the porous scaffold. The penetration and the proliferation of the fibroblast into the porous scaffold were observed.

4. Conclusion

Our purpose was to develop a cell compatible, degradable and synthetic polymer for the novel bioprinting area that shows good mechanical properties and biocompatibility. This polymer must be water soluble and show a rapid phase change or a sol-gel transition so that one can fabricate precision designed scaffolds, and those scaffolds overcome the shortcomings of natural materials such as low mechanical properties, high cost and poor functionality. By incorporation of PCL and sulfonic acid into PU chains, we have synthesized a degradable PU with high elasticity, anticoagulation property, and pH sensitivity in water solution. Due to the pH sensitivity,

this PU becomes water soluble in pH higher than 8.7 and insoluble as pH less than 8.7. This property was utilized in printing technique to fabricate two-dimensional scaffolds designed on the computer-designed patterns. The scaffolds exhibited particular primary and secondary porous microstructures, which may allow the cell attachment and proliferation. Furthermore, the good elasticity, anti-platelet adhesion property of this PU, combined with inkjet printing technique, may further extend the ink-jet printing technique in vascular tissue engineering area.

Part II: chapter 5

LOADING DEPENDENT SWELLING AND RELEASE PROPERTIES OF NOVEL BIODEGRADABLE, ELASTIC AND ENVIRONMENTAL STIMULI-SENSITIVE POLYURETHANES

Abstract

A novel degradable, elastic, anionic, and linear polyurethane was synthesized from hexamethylene diisocyanate, polycaprolactone diol, and a bicine chain extender. The chemical structure, mechanical properties, degradation rate, and swelling ratio were characterized by comparing the polymer with a polyurethane containing a 2,2-(methylimino) diethanol chain extender. Due to the incorporation of negatively charged carboxyl side groups, the bicine extended polymers exhibited higher microphase separation, better mechanical properties in dry condition, and better sensitivity to environmental stimuli than controls, as demonstrated by its high swelling ratio at elevated pH, lower ionic strength, or higher temperature. The swelling ratio of membranes showed reversible change as the function of pH at 37 °C, the membranes becoming fully water-soluble at pH above 8.3. Nile blue chloride and lysozyme were selected to study their release from this polymer. The release rates of both compounds were significantly influenced by the pH and ionic strength. The swelling ratios were also influenced by lysozyme loading at low pH. The pH dependent properties were used to fabricate scaffolds by drop-on-demand printing. Bicine extended polyurethanes may be of interest for possible drug delivery applications, customizable scaffold fabrication and o˙ potential biomedical applications.

1. Introduction

Stimuli-sensitive polymers have received much attention in recent for their potential in a broad range of biomedical devices such as in drug delivery systems, tissue engineering scaffolds, separation membranes, artificial muscles, biosensors, clinical diagnostics, soft actuators, and energy transfusing devices [113-115]. Examples of these polymers include poly(acrylic acid) (PAA), poly(N-isopropylacrylamide) (PNiPAM), poly(ethylene oxide)-co-poly(propylene oxide) (PEO-co-PPO), alginate, fibrinogen, and chitosan; all of which can exhibit reversible changes in their physical properties. Polymers with environmental stimuli-sensitivity that have been fabricated into nano- or micron- sized particles have been shown to be effective injectable drug delivery devices [116-120], by modulating the immune response, extending the circulation time and maintaining the bioavailability of the therapeutic drugs [121-123]. Furthermore, these polymers are attractive because of their predictable drug release kinetics responding to specific physiological conditions [124-127]. In addition, pH-sensitive polymers are particularly attractive for targeted drug delivery applications due to various pH values in different tissue within the body.

Anionic polymers containing carboxylic acid groups, such as carboxylated chitosan, poly(acrylic acid) and its derivatives comprise a family of pH sensitive hydrogels that have been extensively studied for controlled drug delivery, as well as for scaffold fabrication [118, 128, 129]. However, there are many potential limitations of

these polymers as drug carriers such as their poor flexibility, non-degradability, low chemical versatility, immunogenicity, and high cost [130].

In recent years, low-cost ink-jet printing technique has emerged as a novel scaffold fabrication method to precisely control the matrix architecture by using computer-aided imaging design techniques [131, 132]. This technique makes it possible to produce constructs with customized size and shape, allowing tissue engineering grafts to be tailored for specific application or individuals. Moreover, it allows the simultaneous and precise delivery of quantified scaffolding materials, living cells, nutrients, therapeutic drugs, growth factors, and other bioactive components to form cells/scaffold constructs for in vitro and in vivo growth [91, 133-136]. However, there are some limitations in the selection of suitable ink. The inks must be biocompatible, economical, water soluble, and easily solidified to form scaffolds after printing by phase change or crosslinking [133]. Due to poor mechanical properties of the scaffolds printed from natural polymers, the development of printable synthetic biomedical polymers will prove extremely beneficial for precision fabrication of scaffolds with good mechanical strength.

Because of the biocompatibility, chemical versatility, and excellent mechanical properties, non degradable polyurethanes (PUs) have been extensively used in various implantable devices [34, 137, 138]. During the past several years, there has been an increasing interest in design of biodegradable PUs with improved mechanical flexibility compared to most other natural or synthetic biodegradable polymers [73, 75, 139, 140]. However, very little attention has been paid to the synthesis of biodegradable and environmental stimuli-sensitive PUs for biomedical applications and no application for

drug delivery systems or scaffold fabrication by ink-jet printing technique has been reported.

In order to obtain the linear PUs with environmental stimuli-sensitivity, the incorporation of ionic groups into PUs looks promising. Some researchers have reported the synthesis of ionized nondegradable PUs containing sulfonic or carboxyl groups for the application of blood-contacting materials [78, 141]. In those studies, the choice of the hard segment (either aromatic diisocyanate or methylene dicyclohexyl diisocyanate) resulted in low hydrophilicity and low environmental stimuli sensitivity of the polymers, which limited their uses for controlled drug delivery or scaffold fabrication.

Based on the above consideration, our aims of the present study were:

(1) To synthesize a degradable and environmental stimuli-sensitive polyurethane by using a flexible hard segment (hexamethylene diisocyanate (HDI)), a degradable soft segment (polycaprolactone diol), and an ionizable chain extender (bicine). The effects of the chain extender on physical and chemical properties were evaluated in comparison with a polymer synthesized with the same hard segment and soft segment but with a non ionizable chain extender (2,2-(methylimino) diethanol (MIDE));

(2) To study the swelling behavior of the polymers as a function of environmental pH, ionic strength, and temperature. A model compound of Nile blue chloride (NBC) with low molecular weight and a protein, lysozyme, with high molecular weight were selected for investigation of in-vitro release as function of pH and ionic strength. The bioactivity of the released lysozyme was also investigated; and

(3) To modify the polymer into water-soluble polymeric ink for the scaffold fabrication by ink-jet printing.

2. Materials and Methods

2.1. Materials

HDI, bicine, and NBC were obtained from VWR International Company. Dimethyl sulfoxide (DMSO), hydrochloric acid, sodium hydroxide, calcium chloride, potassium chloride, and lysozyme from egg white were purchased from Fisher Scientific International Company. Stannous octoate ($Sn(oct)_2$, $Sn[CH_3(CH_2)_3CH(C_2H_5)COO]_2$) and polycaprolactone diol with M_n=530 (PCL530) were purchased from Sigma-Aldrich (St. Louis, MO). MIDE, dichloromethane (CH_2Cl_2), and N,N-dimethylformamide (DMF) were purchased from Acros Organics Fine Chemicals (Geel, Belgium). Tecoflex was purchased from Lubrizol Corporation (Ohio, USA). HDI was purified through vacuum distillation. BES was vacuum dried at 60^oC for 48 hours before use. MIDE was distilled with calcium hydrogen (CaH_2) to eliminate moisture. DMSO was distilled over CaH_2 at atmospheric pressure under nitrogen protection. PCL530 was dehydrated in a vacuum oven at 60^oC for 48 h. $Sn(oct)_2$ was purified over 4A° molecular sieve using overnight stirring to eliminate trace water prior to use. Lysozyme, NaOH, KCl, and $CaCl_2$ were used without further purification.

2.2. PUs synthesis and membrane preparation

The polymers used in this study were synthesized by the traditional two-step method under nitrogen protection [34]. Briefly, in the first step, stoichiometry of the

reaction was approximately 2:1:1 of hard segment (HDI)/soft segment (PCL530)/chain extender (Bicine or MIDE). The HDI was dissolved in DMSO in a four-neck flask, and PCL530/DMSO solution containing 1%wt $Sn(oct)_2$ as catalyst was added drop wise at 75^{o}C. This mixture was allowed to react for 3 hours before beginning the second step of adding the chain extender.

Because the different chain extenders were used for the synthesis of the two PUs, there were some differences in the process of adding the chain extender at the second step. For the synthesis of the bicine extended PU, 5% w/v bicine dissolved in 90^{o}C DMSO was added into a prepolymer solution. The reaction solution was stirred vigorously, while the reaction temperature was maintained at 90^{o}C for 20-30 min. The reaction solution was cooled down to room temperature, and the chain-extending reaction was allowed to continue for another 10 hours. For the synthesis of the MIDE extended PU, the prepolymer solution was cooled down to room temperature after the first step, and then 5% w/v MIDE in DMSO was added drop wise to the prepolymer solution under intense stirring and room temperature for another 10 hours. After the reaction was finished, the polyurethane solution was precipitated into deionized water for at least 48 hours, dried in the lab hood overnight at room temperature, and then dried in a vacuum oven at 50^{o}C for another 48 hours before further use and characterization.

The sample nomenclature and composition of all the polymers are designated as follows: the first letter denotes the hard segment type (H=HDI), the second letter and number denote the soft segment and its molecular weight (P530=PCL diol with molecular weight 530), and the final letter denotes the chain extender (B=Bicine and M=MIDE). As shown in Fig.1, HP530B symbolizes the PU with molar ratio of 2:1:1

MDI, PCL with molecular weight 530 and BES as the chain extender, while HP530M symbolizes the PU with MIDE as the chain extender.

Synthesized PU membranes were prepared by casting 8% (w/v) PU/DMF solution into a Teflon mold and drying at 60^{o}C for 24 hours. Tecoflex® membranes were prepared by casting 8% (w/v) CH_2Cl_2 solution into a Teflon mold and drying at room temperature in a chemical hood for 4 hours while covered by class plates to prevent formation of bubbles and surface defects. All the cast films were removed from the mold and further dried in a vacuum oven at 60^{o}C for 48 hours to remove residual solvent. The thickness of the obtained membranes was measured by micrometer caliper; the membranes had an average thickness of about 0.15-0.20 mm and were stored in a desiccator at room temperature. The membranes were punched into appropriate size and used for mechanical testing, water swelling behavior analysis, release assays, and in-vitro degradation assays.

2.3. Bulk property characterization

The molecular weights of the synthesized polymers were determined by gel permeation chromatography (GPC; ThermoFisher Scientific, Waltham, MA). The GPC data were calibrated with polystyrene standards (EasiCal PS-1, PolymerLabs, Amherst, MA) with molecular weights in a range of 580-7,500,000 Da. DMF was used as an eluting solvent. The polymers were dissolved at 0.25% (w/v) in the GPC carrier solvent (pure DMF), and 20 μL samples were injected.

Reflective-Fourier transform infrared spectroscopy (FTIR, Nicolet IR200) was used to characterize the chemical structure of synthesized PUs. Sixty-four scans at a resolution of 2 cm^{-1} were averaged. The samples for infrared analysis were prepared by solution casting of 8% (w/v) polymer in DMF directly onto KBr crystal plates and vacuum drying at 60^{o}C for 24 hours prior to characterization.

Thermal analysis was performed in a Mettler Differential Scanning Calorimetry (DSC) analyzer (DSC 822e), with a heating rate of 20 ^{o}C/min, under constant nitrogen flow. Polymer samples were annealed at 50 ^{o}C for 10 min, then cooled down to -100 °C, maintained at this temperature for 10 min, and then tested over the range from -80 to 180 ^{o}C. The weight of each sample was between 70-90 mg.

Tensile tests were conducted using an Instron 4502 at a crosshead speed of 25 mm/min with maximum load of 10 kN. Each sample was cut into approximate 5.5×12 mm^2 rectangular strips. Due to the application of polymers in water-rich environment such as culture media, measurements of the mechanical properties were made in dry conditions and wet conditions with different pH values. Wet samples were prepared by saturating the membranes in phosphate-buffered saline (PBS) with a pH of 7.4 or pH of 5.1 for 12 hours at room temperature to reach equilibrium. Three samples of each condition were measured, and the average tensile strength, elongation, and standard deviation values were obtained.

2.4. Swelling behavior study

For the investigation of environmental pH effects on the dynamic and equilibrium swelling ratio, the polymer membranes were allowed to swell in PBS buffer solution with different pH values at 37 ^{o}C. The surface water was gently wiped with lab-filter paper before weighing at each time point. For the investigation of equilibrium swelling ratio as a function of solution ionic strength at different pH levels, the polymer membrane samples were allowed to swell in KCl solution with different concentration and pH levels (5.5 - 7.4) for at least eight hours until swelling equilibrium was reached. The effects of environmental temperature on membranes' equilibrium swelling ratio were studied by measuring the swollen sample's weight in PBS (pH=7.4) solution at the temperature of 4, 24, 37 and 45 ^{o}C, the samples were allowed to swell for eight hours until they reached the swelling equilibrium before weighing. The swelling ratios were calculated by the weight increase of the swollen samples and initial dried samples according to the equation: swelling ratio = $100\%*(W_s-W_d)/W_{d,}$ where W_s and W_d are the weight of the sample in the swollen and dry conditions respectively. Three samples of each PU were measured to obtain the mean water swelling ratio.

2.5. In vitro degradation assay

In vitro degradation of the PUs was evaluated by recording the samples' weight losses over time in PBS buffer solution at 37^{o}C. Each round-shaped PU sample punched from the dry membrane had an initial weight of approximately 5 mg and a size of 4.5 mm in diameter and 0.16 mm in thickness. The samples were placed in small vials that were

separately filled with 1 ml PBS (pH=7.4) buffer solution containing 0.5% (W/V) sodium azide. Those vials were then placed in a 37^{o}C water bath with cyclic shaking to simulate in vivo dynamic tissue environment. At each time point of Weeks 1, 2, 3, 4, 5 and 6, each of the vials were sampled, rinsed for 1 hour by deionized water, and vacuum dried for 48 hours before weight loss analysis. The PBS solution in each vial was also collected for pH value measurement. After that, the PU samples were put back into vials, and 1 ml fresh PBS (pH=7.4) buffer solution was added into each vial.

2.6. Loading and release studies

Solutions were prepared by dissolving NBC (1mg/ml) or lysozyme (10mg/ml) in pH 7.4 PBS buffer solution. The PU membranes containing carboxyl groups were punched into round-shaped samples 4.5 mm in diameter and 0.16 mm in thickness. These round samples were then immersed in the NBC or lysozyme aqueous solution, and the complexation reaction was allowed to proceed at 37^{o}C for 2 days. The PU samples were washed extensively with deionized water at room temperature six times to remove any loosely-bound compounds. The loading percentage of lysozyme in PU was determined by weight change after vacuum drying, according to the equation: lysozyme loading rate = 100%*(W_l-W_d) /$W_{d,}$ where W_l indicates the weight of dried lysozyme complexed PU, and W_d indicates the initial weight of the PU sample. The loading rate of the lysozyme in the HP530B hydrogel at pH 7.4 and 37^{o}C was 33.2±3.3%, indicating a high lysozyme loading efficiency. Each PU membrane loaded with lysozyme was immersed in 0.5 ml of different pH PBS solutions or different KCl solutions at 37^{o}C. At each time point, 0.4 ml

solution was taken out, and the concentration of lysozyme was determined by measuring UV absorbance at 280 nm with a spectrophotometer (μQuant, Bio-Tek Instruments, Inc.). Three samples of each PU were measured to obtain the mean value and standard deviation.

The enzymatic activity of released lysozyme was determined by EnzChek® Lysozyme Assay Kit (Invitrogen, Atlanta, GA). The samples solution containing released lysozyme was diluted 10-fold with the buffer (pH 7.5) containing 0.1 M sodium phosphate and 0.1 M NaCl. 50 μl of the sample solution was mixed with 50 μl of lysozyme substrate working buffer suspension, which contained 50 μl/ml Micrococcus lysodeikticus labeled with fluorescein. This mixture was allowed to incubate for 30 minutes at 37^{o}C with protection from light. The lysozyme acted on the cell walls causing the release of the quenched fluorescent substance. The fluorescence increase was measured using a spectrophotometer (Molecular Devices Corp.) with the fluorescence absorption at 494 nm and emission at 518 nm. An increase in fluorescence strength, which was attributed to the degradation of the substrate, corresponded with the lysozyme activity. The purchased lysozyme was diluted into 10 μg/ml in PBS buffer solution and used for comparison.

2.7. PU dissolution and scaffold fabrication

PU dissolution was carried out by dissolving HP530B into 1 M NaOH water solution at room temperature to form 25% (w/v) aqueous polymer solution; the pendant carboxyl acid groups on polymer chains were reacted into carboxyl ions, and the PU

became water soluble. A HP desktop 3900 printer and the HP 21 black ink cartridge were modified to fabricate single-layer patterns, as described elsewhere [132]. A 0.2 M $CaCl_2$ water solution was poured into the cartridge, and the 25% (w/v) aqueous polymer solution was dropped on the glass slide surface to form an even liquid layer. This glass slide was then placed onto the print stage mounted under the printhead. The patterns consisted of letters ("CLEMSON," font: Arial, size: 20). The $CaCl_2$ solution was printed out in two cartridge passes onto the glass slide and reacted with the polymer solution. The printed patterns were then photographed.

3. Results and Discussion

3.1. Characterization of the polymers

Figure 1 shows differential scanning calorimetry (DSC) spectra for two types of PUs. Glass transition temperatures (T_g) of -35 ^oC and -28 ^oC were observed for H530B and H530M. Both PUs exhibited much lower T_g than 37 ^oC, indicating that the PUs are capable of maintaining characteristic elasticity at body temperature. HP530B exhibited a lower T_g value than HP530M, indicating the higher micro-phase separation. This enhanced micro-phase separation can be explained by the existence of the additional carboxyl groups, which caused a significantly higher polarity difference between the hard segments and soft segments in HP530B. The endothermal melting peaks at 71 ^oC and 64 ^oC indicate the HDI-based polyurethanes are crystalline indicating that the aliphatic chains of HDI and PCL in the hard and soft segments are easily aligned in an orderly

configuration. The higher melting point of HP530B can also be explained by its higher micro-phase separation, which further increases alignment in the crystallized areas.

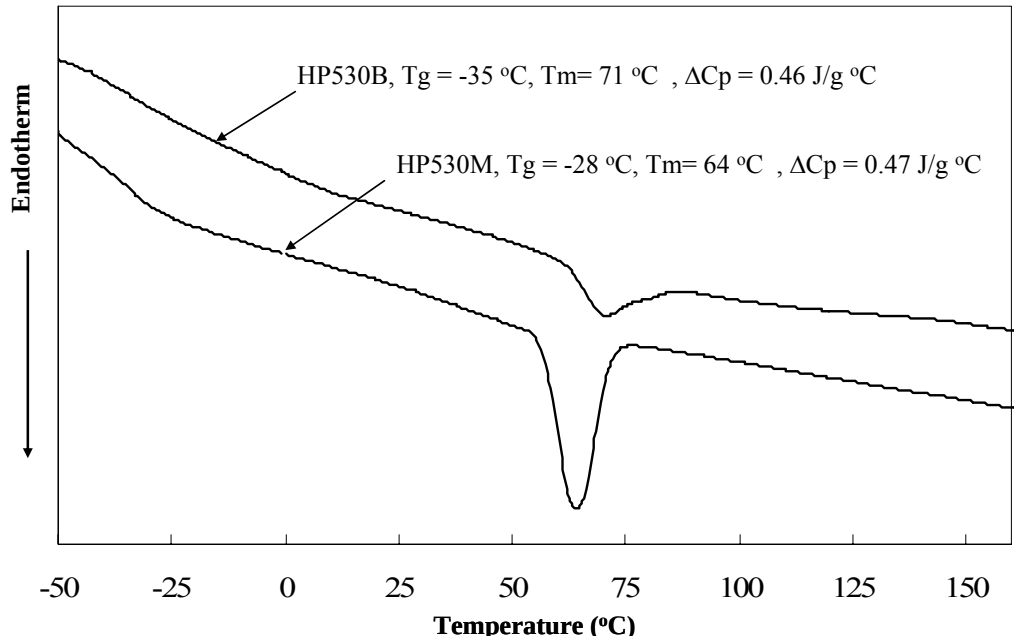

Figure 1: DSC thermograms of two types of biodegradable PUs of HP530B and HP530M. The curve on the top shows the thermal behavior of HP530B with T_g at -35 ^oC, T_m at 71 ^oC and ΔC_p of 0.460 J/g ^oC. The curve on the bottom shows the thermal behavior of HP530M with T_g at -28 ^oC, T_m at 64 ^oC and ΔC_p of 0.470 J/g ^oC.

Figure 2 shows the FTIR absorption spectra of the HP530B and HP530M at room temperature. Because both PUs were synthesized at the same stoichiometric molar ratio of the hard segment, the soft segment, and the chain extender (as shown in Table 1), the FTIR spectra exhibited substantial similarity to each other between the wavelengths of 400 - 4000 cm^{-1}. HP530B demonstrated an extra absorbance peak at approximately 1640 cm^{-1}, which indicates the symmetric stretching of pendant carboxyl group on the polymer backbone and shows the successful incorporation of the carboxyl groups (as shown in the illustration of chemical structures in Figure 2). Furthermore, the C=O stretch region can provide useful information on the hydrogen bonding mode of the carbonyl groups in the

PU, by calculating the ratio of the hydrogen bonded carbonyl group absorbance at 1706 cm^{-1} to the free carbonyl group absorbance at about 1730 cm^{-1} [78, 142]. This ratio of bonded carbonyl to free carbonyl of HP530B and HP530M is about 0.98 and 1.01, respectively. The lower ratio is observed in HP530B because the incorporation of the bicine provided more free carbonyl groups.

Table 1: Composition, molecular weight and mechanical properties of biodegradable PUs made from HDI, PCL530 and chain extender of bicine or MIDE. Commercial PU of Tecoflex was used as a control for the comparison of mechanical properties.

	Composition	GPC	Mechanical Properties					
			Tensile Strengh (MPa)			Elongation (%)		
			Dry	Wet		Dry	Wet	
Materials	Molar ratio	Mn (g/mol)		pH=5.5	pH=7.4		pH=5.5	pH=7.4
HP530B	HDI/PCL/Bicine 2/1/1	106,000	5.8 ± 0.4	2.2 ± 0.5	0.4 ± 0.1	754.6 ± 128.3	1448.9 ± 80.8	661.0 ± 57.1
HP530M	HDI/PCL/MIDE 2/1/1	92,600	1.3 ± 0.5	0.4 ± 0.2	-	100.3 ± 8.5	18.0 ± 7.0	-
Tecoflex	-	-	28.1 ± 4.9	-	-	345.8 ± 66.6	-	-

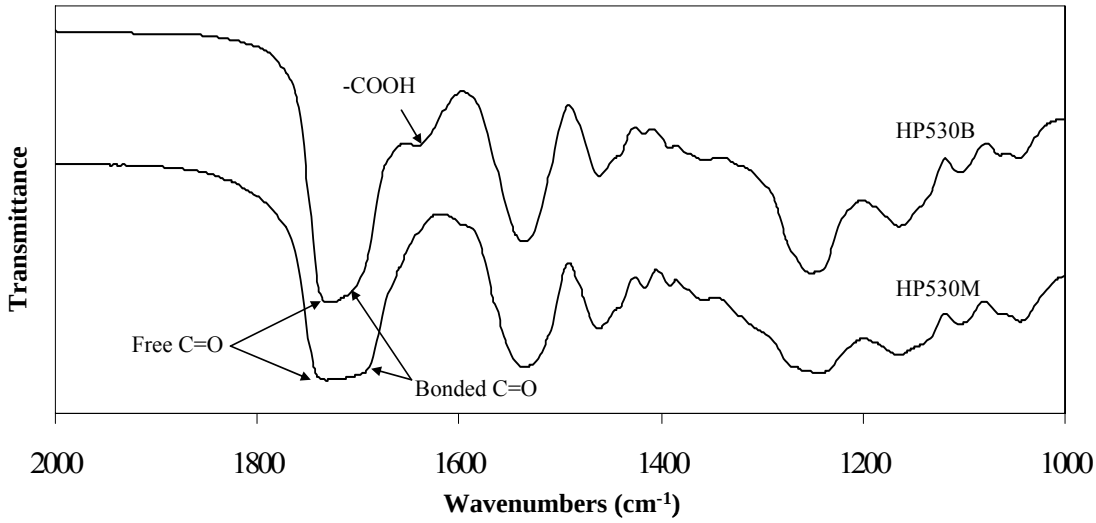

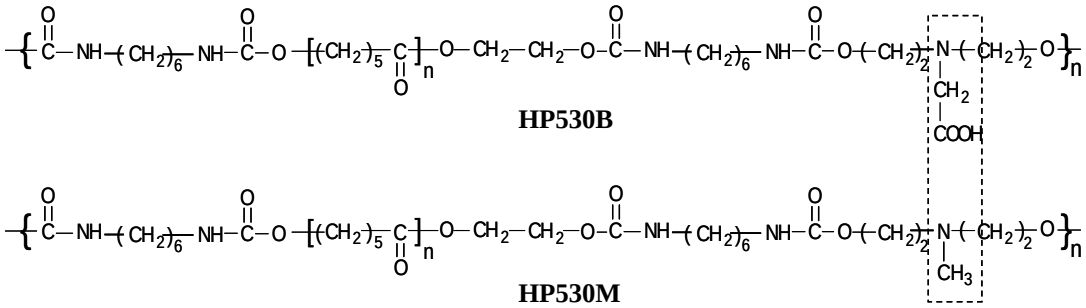

Figure 2: FTIR spectra of the PUs with different chain extenders. The bands at 1640 cm^{-1} corresponds to the symmetric stretching mode of -COOH, the bands at 1730 cm^{-1} and 1706 cm^{-1} correspond to the stretching mode of the hydrogen bonded carbonyl group and free carbonyl group respectively. The ratio of bonded carbonyl absorbance to free carbonyl absorbance of HP530B is about 0.98 and same ratio of HP530M is about 1.01, indicating higher percentage of free carbonyl groups in HP530B. The chemical formulas of the polymers are also shown.

The tensile strength and elongation values of HP530B and HP530M samples are compared in Table 1. The commercial Tecoflex™ polyurethane containing linear polytetramethylene oxide (PTMO) in soft segment was selected as a control. Compared to the HMDI-based Tecoflex, both HP530B and HP530M exhibited much lower ultimate tensile strength in dry condition due to the ester group in the soft segments and the side groups in the chain extender, the groups undermine the orderly alignment of the polymer

matrix, and therefore decrease the mechanical properties. However, because the aliphatic HDI in hard segment provided a linear and flexible structure in the hard segment of the HDI-based PUs, the HP530B exhibited much better elongation than Tecoflex. In comparison to HP530M, HP530B showed better mechanical properties in dry and wet conditions at a pH level of 5.6. This can be explained by two reasons. First, the incorporation of the polar carboxyl groups in the polymer matrix caused the formation of the ion aggregates that served as extra physical crosslinks. These crosslinks increased the micro-phase separation and enhanced the interaction among polymer chains. Secondly, the relatively low molecular weight of HP530M (approximately 1/10 of HP530B) caused the dramatic decrease in chain entanglement and chain interactions.

As mentioned in other paper[39], the mechanical properties of the polyurethane, which was synthesized from butane dissocyanate (BDI), PCL and butanediamine, exhibited tensile strength at approximate 25 MPa and elongation at 600 % according to ASTM D638-98 . Although the different testing method is used for HP530B, we can roughly compare two polyurethanes. HP530B showed similar elongation value but lower tensile strength. The lower tensile strength can be explained by the lower hydrogen bonds density in HDI based polyurethane, which is caused by longer HDI chain than BDI and lower hydrogen bonds interaction from chain extender bicine than that from butanediamine.

After saturation with PBS buffer solution at pH 7.4 and 5.6, an obvious drop of the tensile strength was found for both HDI-based PUs. The tertiary nitrogen atoms in the chain extender of HP530M and carboxyl groups in the chain extenders of HP530B have

certain polarity, which resulted in the formation of the hydrogen bonds of these groups with water in the solution, thereby undermining the interactions among the polymer chains and decreasing the polymer tensile strength. Among two types of PU, the mechanical properties of HP530B showed pH dependent, as shown in Figure 3, the mechanical properties decreased with the increase of the media pH (5.6 to 7.4), while HP530M exhibited negligible mechanical property changes after being saturated by the buffer solution at different pH levels. The change in mechanical properties of the HP530B as a function of the solution pH can be attributed to the changed hydrophilicity of the polymer matrix. At high pH value, the carboxyl groups on the polymer chains were deprotonized and partially became soluble in water, which enabled HP530B to become hydrophilic at high solution pH. Therefore, the tensile strength of HP530B in water decreased with the increase of the solution pH. However, in comparison to the dry HP530B, the elasticity of wet HP530B samples in different pH solution showed improved or similar values at pH 5.6 and 7.4 without obvious yield points. This can be explained by the role of water molecules serving as ‘lubricant’ among hydrophilic polymer chains, so the polymer chains became more flexible and extendible in hydrophilic condition. This property may be useful for biomedical applications that demand highly elastic materials such as artificial blood vessel, heart valve, artificial skin and other implants for soft tissues engineering.

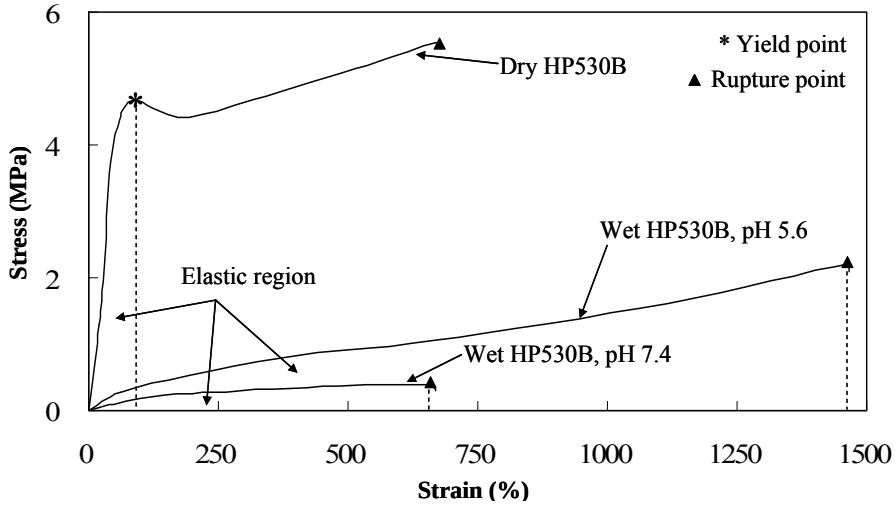

Figure 3: Typical stress-strain curves of HP530B in dry condition and wet condition saturated with PBS buffer solution with pH at 5.6 and 7.4, respectively. * indicates the yield point of the sample under stress, ▲ symbol indicates the rupture point of the sample. In wet conditions, HP530B shows lower tensile strength but a wider elastic region than dry ($P<0.05$). With the slight increase of the buffer pH from 5.5 to 7.4, the samples mechanical

3.2. In vitro degradation assay

Both HP530B and HP530M contain large amounts of ester and urethane groups in the hard and the soft segment that can be hydrolyzed in the water into small molecules such as hexanediamine, caproic acid, bicine or MIDE, which are known to accelerate the hydrolysis. Initially, the polymer matrix maintains most of its initial weight because of the insolubility of the degraded polymer chains. However, as the hydrolysis progresses, the short polymer chains are degraded into water-soluble molecules. HP530B and HP530M both showed in-vitro degradability. The degraded polymer matrix fragments could be easily dissolved by DMF, indicating that the polymers still retained their linear structure without crosslinked side reactions during degradation. Figure 4 shows that HP530M lost approximately 4% of its initial weight compared to a 2% loss for HP530B. The higher weight loss rate of the HP530M is attributed to its lower phase separation

degree and low molecular weight. Although HP530B has higher hydrophilicity due to the ionization of carboxyl groups in buffer solution, we hypothesize that its high-microphase separation enhanced the interaction force among the polymer chains, thus resisting water attack. The pH of the degradation solution of HP530B was consistently lower than that of HP530M by 0.1 (see Figure 4) which we attribute to the pendent carboxyl groups. Given the relatively stable pH of the degrading solution around 7.2, we expect the degradation products to not significantly influencing the pH in vivo.

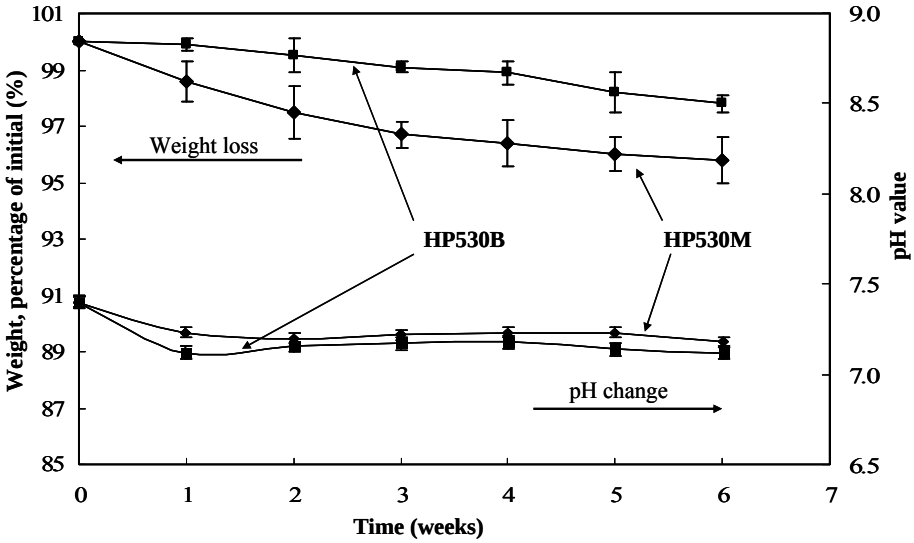

Figure 4: Degradation behavior of two types of PUs in PBS buffer solution at 37 °C: The average retained weight of HP530B and HP530M change as a function of weeks in PBS. The pH values of degradation solution during degradation are also shown.

3.3. Swelling behavior study

The ability of ionic hydrogels to transition, in response to environmental stimuli, from a swollen to a collapsed configuration or vice versa is important for various biomedical applications. For example, hydrogels have been investigated as the reservoir system for insulin release, where the shrinkage in the hydrogel leads to the release of entrapped insulin through the membrane [143]. Different mechanisms, such as diffusion,

swelling, the squeeze effect, and the ionic interaction [144, 145], have been proposed to explain drug release from hydrogels. HP530B membranes were tested in various buffer solutions at different pH values, ionic strengths, and temperatures to investigate the swelling behavior of the HP530B (see Figure 5). We found that the HP530M showed very low environmental stimuli sensitivity (5% swelling ratio independent of pH) while HP530B exhibited a swelling ratio of approximately 140% at the pH 7.4. At higher pH the swelling ratios increased in a linear manner, which is attributed to continuous deprotonation of the carboxyl acid groups until the hydrogel's pK_a of 8.3, which is close to that of bicine, is reached. This is expected as, in ionic hydrogels, the water absorption rate is controlled by both diffusion and polymer chain separation [146], which increases due to electrostatic repulsion the more carboxylic acid groups of the bicine become ionized. Figure 5A shows the equilibrium swelling ratio of HP530B at pH values ranging from 3.0 to 9.0. The ratio varies from 25% at pH 3.0 to 140% at pH 7.4 to 350% at pH 8.0. At pH above 8.3 the hydrogels dissolved. However, in a low pH range from 3.0 to 6.2, the equilibrium swelling ratio showed little if any change and stayed at 25%.

The effect of the cyclic change of the pH on the swelling behavior of the H530B was investigated, and the results are shown in Figure 5B. When the pH level changed cyclically from 5.1 to 7.4, the water swelling ratio kept changing reproducibly between 40% and 140%. When the pH was increased from 5.1 to 7.4, it took approximate 2 hours for the swelling ratio of HP530B changed from 40% to 150%; as pH was decreased from 7.4 to 5.1, the swelling ratio changed from 150% to 40% within 1.5 hours. These results indicated that HP530B has a reversible and quick pH response. This is attributed to

charge repulsion between chains due the deprotonation and protonation reactions as explained above coupled with the linear structure of this polymer rather than crosslinked structure as in other pH sensitive hydrogels. It is also found that the de-swelling rate was 2-3 times higher than the swelling rate. This is likely due to the different mesh size of hydrogel at the pH levels of 7.4 and 5.1. The large mesh size of the hydrogel matrix network allowed an easy diffusion of solute into matrix and reaction with the carboxylic groups.

The equilibrium swelling ratio of the HP530B as a function of ionic strength was measured at a pH levels of 7.4 and 5.5 in KCl solution (37 ^{o}C). The salt concentration was changed from 0 to 1.0 M. Figure 5C shows that at pH 5.5 the ionic strength did not noticeably affect the equilibrium swelling ratio. However, at pH 7.4 the equilibrium swelling ratio increased dramatically as the ionic strength decreased. The low sensitivity of HP530B at a pH of 5.1 is due to the low ionization degree of the polymeric hydrogel. With the increase of pH to 7.4, the polymer chain became highly ionized, with increased polymeric ion concentration, causing an increase on the polymer osmotic pressure and subsequent water absorption [147, 148]. The influence of the temperature on the equilibrium swelling ratio at pH 7.4 was also studied (data not shown). The equilibrium swelling ratio increased with the temperature from 40% at 4 °C, to 104% at 24 °C, 140% at 37 °C and 240% at 45 °C. The environmental sensitivity of the HP530B may find many applications in the biomedical arena including use as separation membranes, artificial muscles, biosensors, and drug delivery systems.

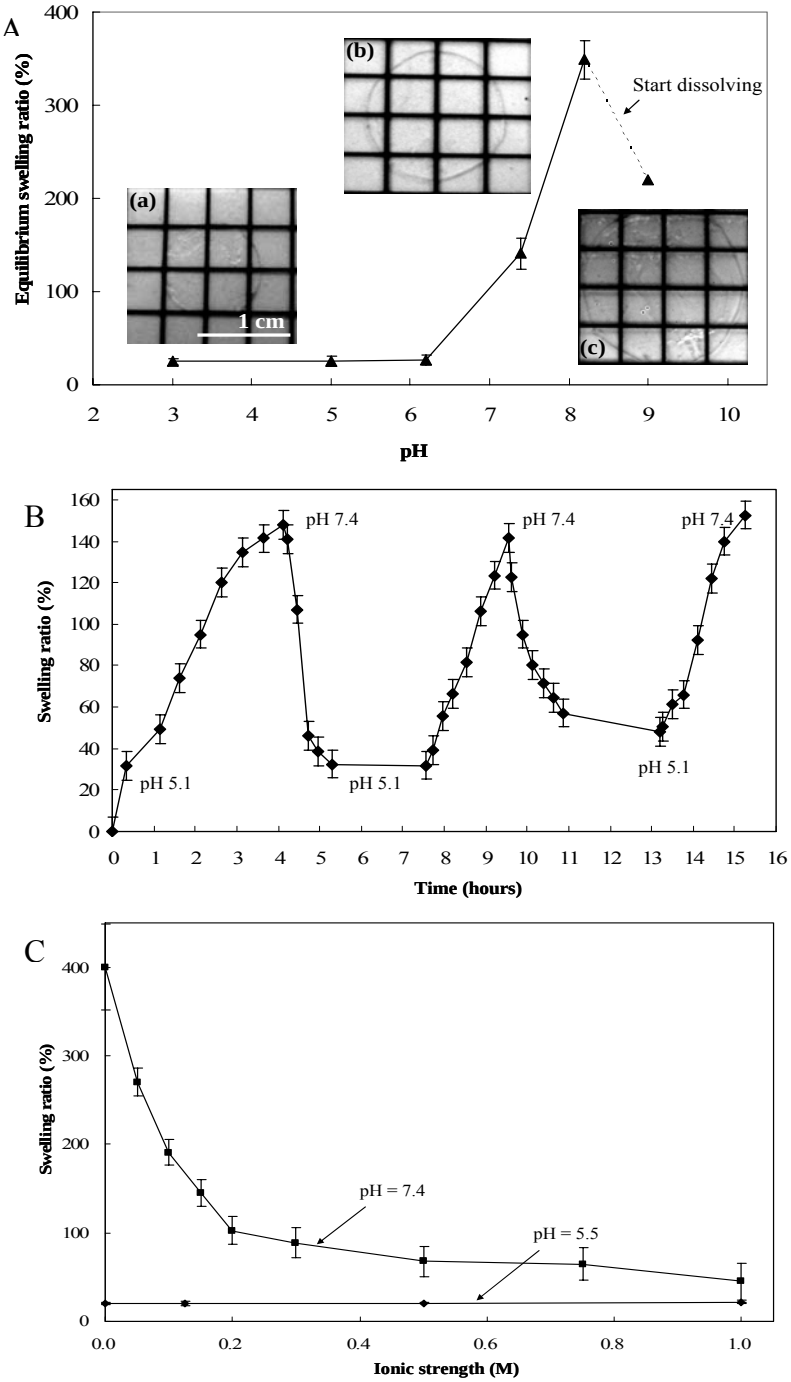

Figure 5: Swelling studies of HP530B as function of pH and ionic strength. (A) Equilibrium swelling ratio of the HP530B as a function of the environmental pH in PBS buffer solution (ionic strength is approximate 0.15 M) at 37 °C. Each sample was saturated in the solution for at least 12 hours before weighed (n = 6, means ± S.D.). The photographs reflect the size change of HP530B membranes at pH = 5.0, 7.4 and 8.2. (B) Cyclic swelling behavior in PBS buffer solution (ionic strength is approximate 0.15 M) with cyclic pH changes between 5.1 and 7.4 at 37 °C (n = 3, means ± S.D.). (C) Equilibrium swelling ratio of the HP530B as a function of the buffer ionic strength at pH 5.5 and 7.4 respectively. Each sample was saturated at 37 °C in the KCl solution with different concentration for at least 12 hours before weighed (n = 3, means ± S.D.).

3.4. Release studies

The release of a low molecular weight dye, Nile Blue chloride (NBC), and the protein lysozyme from the HP530B hydrogels were studied as function of pH. Because of the low polarity of HP530M, the drug amount loaded on HP530M was comparatively small and not studied. At pH 7.4, the HP530B should allow unimpeded penetration of the positively charged molecules into matrix and the further immobilization of the compounds due to the negatively charged polymer chains as illustrated in Figure 6. The cumulative release amount of NBC from HP530B hydrogel into buffer solution at several pH levels is shown in Figure 7A. The highest release rate was observed at pH 8.3, and this rate decreased with decreasing pH down to pH 6.5. For further pH decreases to 5.1, a higher release rate was observed. The swelling ratios at the different pH levels for the NBC-loaded HP530B membranes were the same as those of the pure HP530B membranes The low release of NBC at pH 7.4, where swelling rates are greatest suggests that releases is controlled by electrostatic NBC/COOH interactions rather than diffusion. As illustrated in Figure 6, the positively charged NBC is interacting with negatively charged polymer chains at pH 7.4. Because the hydrogen ions in the solution have a higher electrostatic affinity for carboxyl groups than NBC molecules, the NBC molecules on polymer chains are easily substituted with the hydrogen ions and then allowed to diffuse out of the polymer matrix, a process that is H^+ concentration dependent. At a pH higher than 7.4, when the NBC release is mainly controlled by diffusion as the NBC-loaded hydrogel started to dissolve due to the increased ionization of the polymer chains, and this dissolution then caused the highest NBC release rate at a pH of 8.3. The

association and disassociation of the NBC from hydrogel matrix is dramatically affected by environmental pH, a higher pH causes a lower NBC binding off rate, thus lower amount of NBC is released at a higher pH; however, when pH higher than 8.3, though the binding off rate of NBC and matrix becomes lower, NBC can be released into solution at a high rate in combination with the dissolved polymer chains. The pH dependent release of small compounds will be useful delivery of anticancer drugs such as Adriamycin, Triptorelin, Paclitaxel, and Letrozole, because many of these anti-cancer drugs have a low molecular weight and positively charged groups in aqueous condition, and those drugs need to be released at lower pH ($\leqslant$6.5) of tumor environments [149, 150].

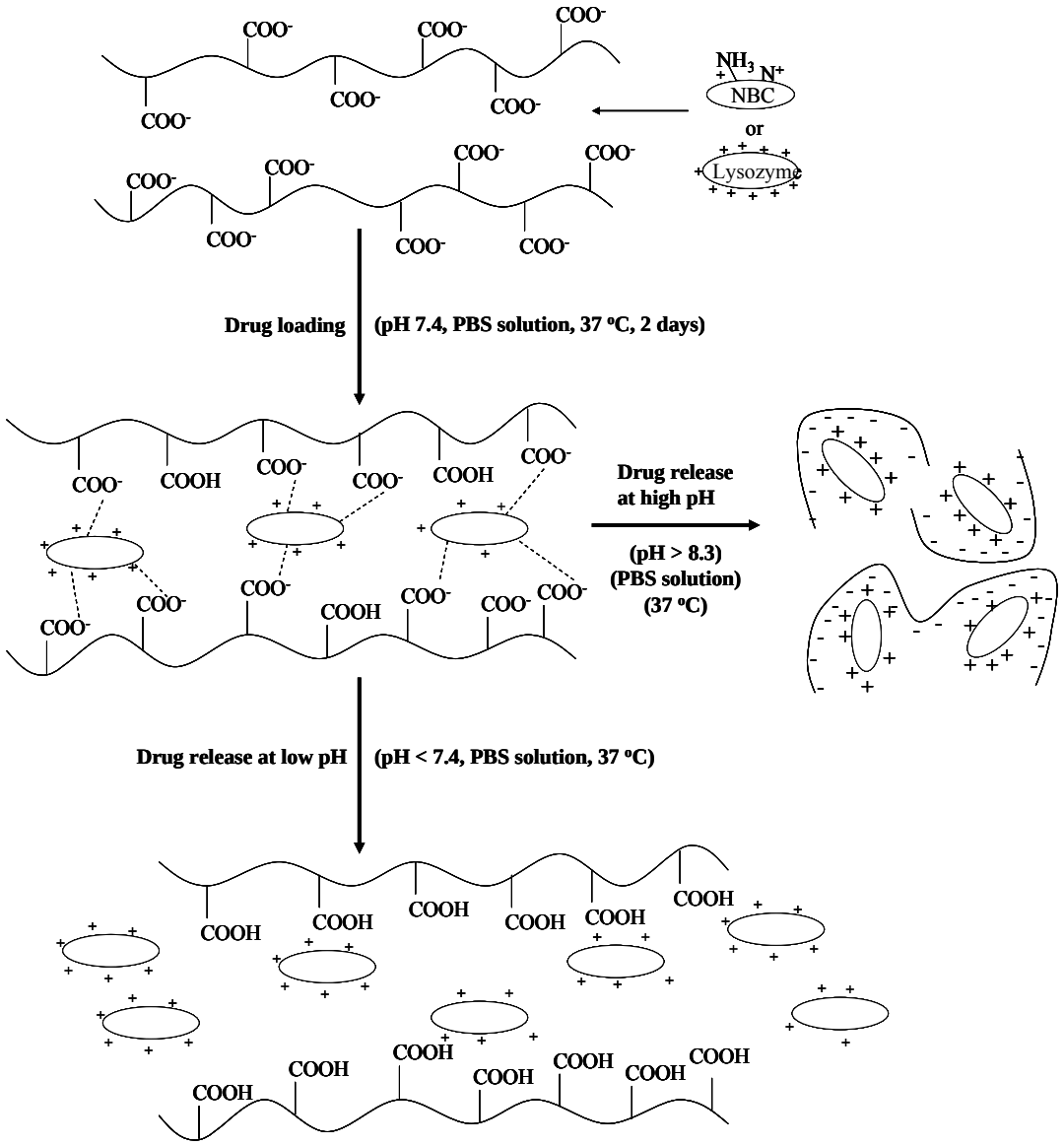

Figure 6: Schematic diagram of complexation reaction of HP530B hydrogel with drug NBC or lysozyme in PBS buffer solution at 37 °C and pH 7.4, and the mechanism of drug release procedure at low pH (<7.4) or high pH (> 8.3). The dotted lines represent the covalent bonds among the negatively charged carboxyl groups on the polymer and the positively charged groups on the drugs. At low pH, the monomer drugs released through chemical substitution reaction; and at pH > 8.3 the drugs were dissolved into solution with the dissolution of hydrogel, covalent bonds between polymer and drugs were not broken.

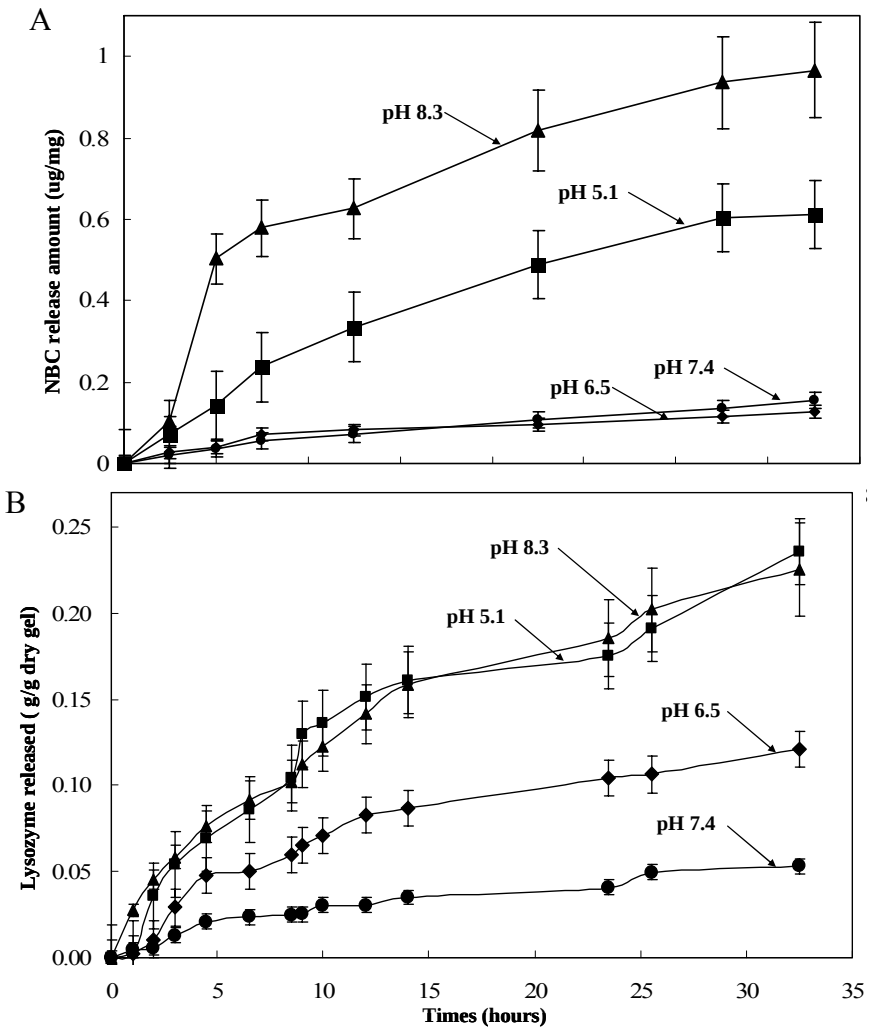

Figure 7: Cumulative amount of model drug released from HP530B at different pH values in PBS solution (ionic strength about 0.15 M) and constant temperature of 37 °C. (A) Release of NBC after priorsaturation in the 1mg/ml NBC buffer solution at pH 8.3, 7.4, 6.5, 5.1 for 8 hours assay (n = 3, means ± S.D.). (B) Release of lysozyme after saturation in 10mg/ml lysozyme buffer solution at pH 8.3, 7.4, 6.5, 5.1 for 2 days assay (n = 3, means ± S.D.).

The release of lysozyme, a protein with an approximate molecular weight of 14 kDa and pK_a of 11, from the HP530B hydrogels at different pH values was studied by measuring the cumulative amount of released lysozyme from the loaded HP530B membrane at different points in time. During the loading process, the transparent swollen hydrogel gradually turned opaque from the surface to the core, and the swelling ratio

decreased from 140% to 83%. The hydrogel still maintained its flexibility after being loaded with the protein. As shown in Figure 7B, lysozyme was released at similar rates at pH 5.1 and 8.3, at lower rates at pH 6.5 and at lowest amounts at pH 7.4. Under acidic conditions, lysozyme release increased with the decreasing pH, indicating that the electrostatic interaction between polymer chains and protein molecules dominate the release. As described above in the case of NBC release, we hypothesize that H^+ ions are substituting for lysozyme which is subsequently released in an H^+ concentration dependent manner. At a pH value higher than 7.4, the polymer chains become highly ionized and the polymer starts to dissolve, releasing a lysozyme-polymer complex at high rates. Because of the positive charge of lysozyme in the solution, the lysozyme binding off rate from hydrogel matrix has similar change as in NBC release. The binding off rate decreases in accordance to the increase of the environmental pH, thus the lysozyme release rate becomes lower at a high pH. At pH higher than 8.3, lysozyme can be released into solution at a high rate in bind with the dissolved polymer chains.

We also found that at pH 5.1, the swelling ratio of the HP530B changed drastically from 30% unloaded to 470% when loaded with lysozyme (Figure 8A). In addition the gels have a white appearance. The swelling ratio reduced to 50% after the lysozyme was allowed to be released at pH 6.5. The swelling ratios at higher pH are largely unchanged for lysozyme loaded versus unloaded gels. NBC loaded gels never showed loading dependent swelling rates.

The loading dependent swelling rates at low pH are attributed to relatively high molecular weight and hydrophilicity of the lysozyme. At a pH of 5.1, most of the

lysozyme in the gel is dissociated (‘free’) from the polymer chains. This lysozyme is still encapsulated in the matrix due to the weak hydrogen bonds between polymer chains and the limited hydrogel mesh size that exists at those pH levels. Due to its hydrophilicity the ‘free’ lysozyme will attract water and cause increased swelling ratios. While at a pH of 6.5 the hydrogel showed the lowest swelling ratio, it can be attributed to the low ionization degree of the hydrogel and to the limited amount of “free” lysozyme in the matrix. As the pH level increased to 7.4, the hydrogel ionization degree increased, which to a certain degree counteracted the decreased amount of “free” lysozyme in the matrix; thus, the swelling ratio was merely slightly higher than that at pH 6.5.

The release of the lysozyme from the HP530B in solutions of different ionic strength at 0.2 M and 0.05 M by KCl was also studied (data not shown). Lysozyme release increased with the increase of the ionic strength. This is a further indication of lysozyme/carboxylic acid interactions. Figure 8B shows the enzymatic activity of released lysozyme at different pH levels in PBS buffer solution and varying ionic strength in KCl solution. The lysozyme released at pH values of 7.4, 6.5, and 5.1 and ionic strengths of 0.05M and 0.2M exhibited slighter lower enzymatic activity than that of free lysozyme. However, at a pH of 8.3, the activity of lysozyme was 32% lower than the control, indicating that lysozyme may indeed be electrostatically coupled with dissolved polymer chains as hypothesized above.

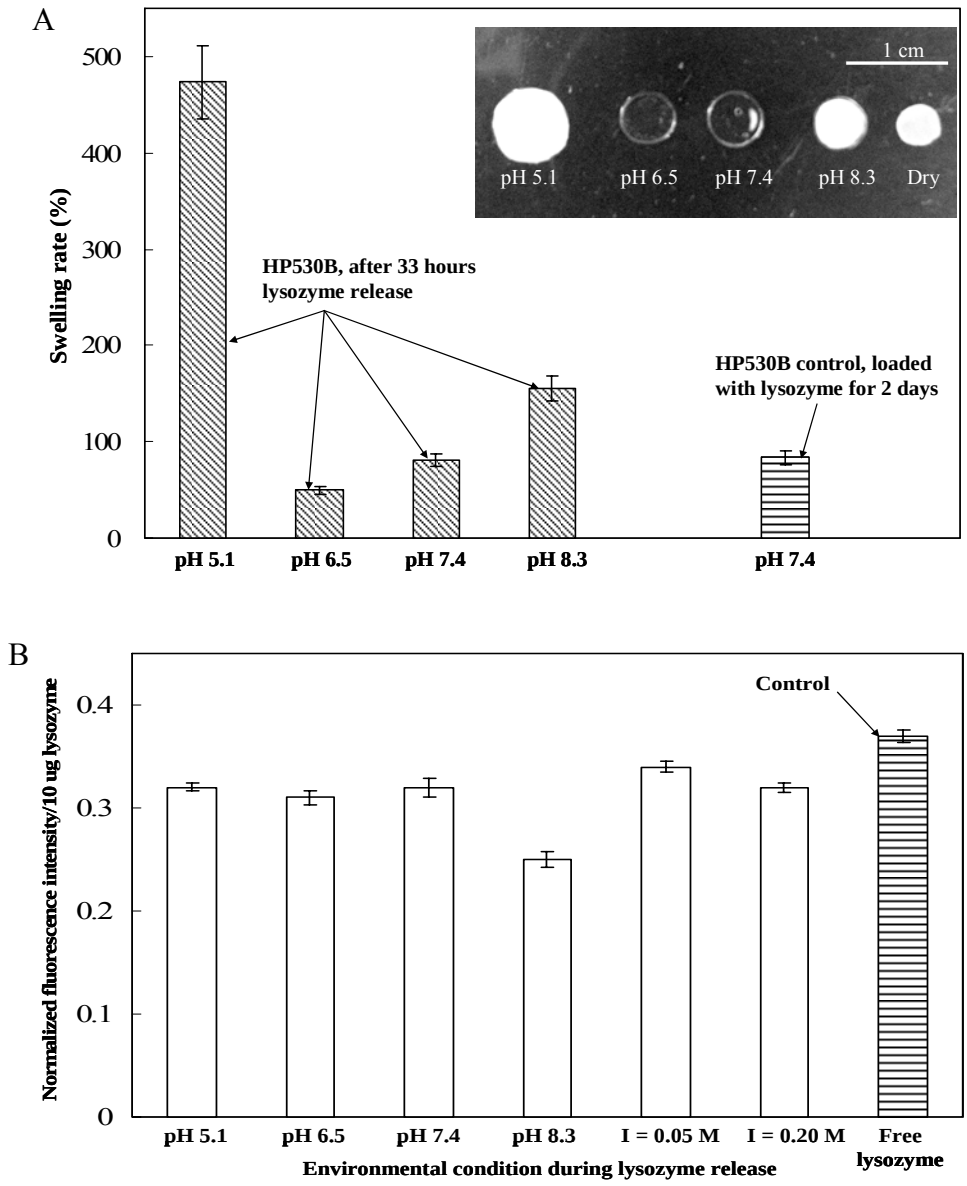

Figure 8: (A) The swelling ratio of HP530B membranes after 33 hours lysozyme release assay at different pH values in PBS buffer solution at 37 °C. HP530B loaded with lysozyme was used as swelling rate control (n = 3, means ± S.D.). The photograph reflects the size of the HP530B membranes after 33 hours release at different pHs. The dry HP530B was used as size control. (B) Lysozyme activity after release from HP530B hydrogel at pHs of 5.1, 6.5, 7.4, 8.3 in PBS solution, and ionic strength in KCl solution (pH 7.4) of 0.05 M, 0.2 M respectively. Free lysozyme dissolved in pH 7.4 buffer (10 μg/ml) was used as control. The fluorescence intensity was recorded after 30 min incubation of lysozyme solution with lysozyme substrate working buffer at 37 °C, it is proportional to the amount of the fluorescent substances that was released by the reaction between biologically active lysozyme and micrococcus lysodeikticus membrane (n = 3, means ± S.D.). I: ionic strength.

3.5. Scaffold fabrication by ink jet printing technology and SEM observation

In order to fabricate drug releasing scaffolds by inkjet printing, we took advantage of the pH sensitivity of the polymer. We chose to print $CaCl_2$ (pH 4.0, 0.6M) onto a fully solubilized polymer solution (pH8.6). Upon the impact of the $CaCl_2$ droplets, the HP530B precipitated onto the glass slide due to local pH change. The precipitated polymer remains insoluble as long as the pH does not increase above 8.4. As shown in Figure 9(A), different letters (CLEMSON) could be printed on identically computer-designed patterns, indicating that the HP530B can be easily used for the fabrication of a scaffold. SEM observation result shown in Figure 9(B) indicated a porous structure is formed after printing. Compared to the scaffold from MP530B, scaffold from HP530B showed relatively irregular porous structure, no secondary porous structure with pore size less than 100 nm can be found. This difference can be explained by the different hydrophilicity between MP530B (about 5%) and HP530B (about 25%) at neutral environment. MP530B formed a hydrophobic scaffold after solidification the polymer chains exhibited low mobility in the matrix, thus the pore structure keep their original condition. In comparison, HP530B formed a gel-like scaffold in neutral environment due to its high hydrophilicity, the polymer chains still maintained mobility in the matrix, thus the porous structure continued merging to each other. This further caused the disappearance of small pores and irregularly distributed large pores in the matrix.

This technique can potentially be adapted to three-dimensional patterns using the method described earlier [133]. Furthermore, the bioactive molecules such as drugs or growth factor could be also encapsulated into scaffold either during printing by adding

drug into cartridge or after printing by immersing scaffold into drug solution. In our lab, the related research on fabrication of drug loaded scaffolds is carried on.

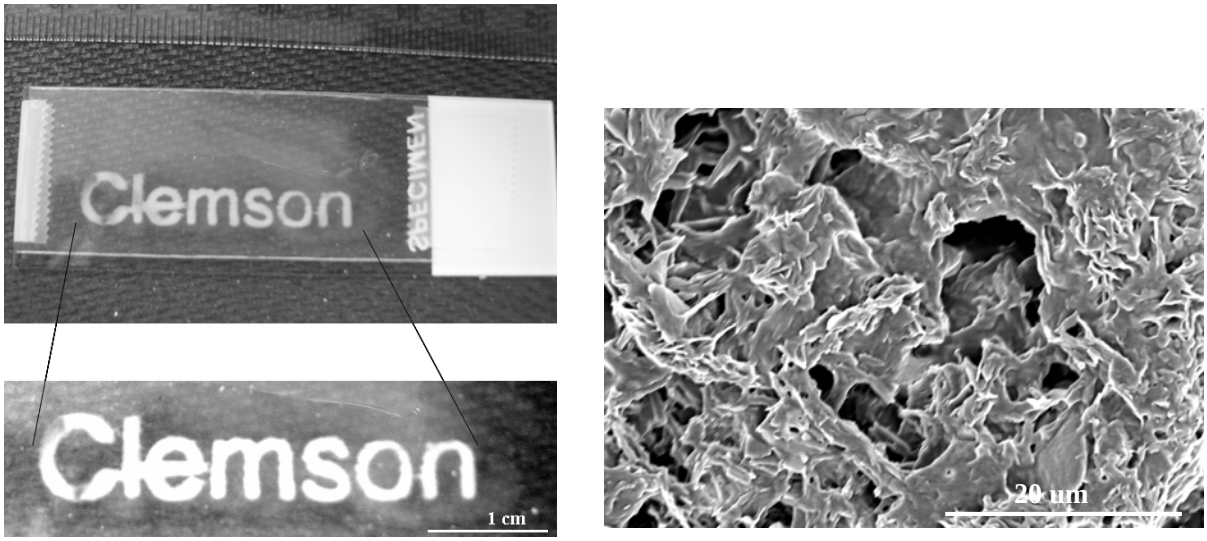

(A) (B)

Figure 9: (A) Two-dimensional patterns printed on the standard glass slides by inkjet printing technique. 0.2 M $CaCl_2$ water solution in HP 21 cartridge was printed out by two passes on 25% (W/V) H530B water solution coated glass slide. Patterns immediately formed in 3 second after printing. All the letters printed in the font of Arial and the size of 20; (B) SEM images of the PU scaffold showing irregular porous structure. Magnification 2500x.

HP530B is studied as drug delivery carrier in this paper. We also want to fabricate the scaffold by ink-jet printing technique; the scaffolds were expected to have drug delivery properties too. The drug can be combined with scaffold either during printing by adding drug into cartridge, or after printing by immersing scaffold into drug solution. So the printed scaffold can be more functional for tissue engineering.

4. Conclusions

In our study, we have successfully synthesized a novel elastic degradable polyurethane with PCL as the soft segment, HDI as the hard segment, and bicine as the

chain extender. By the incorporation of the carboxyl groups onto its linear chain, the polymer exhibited sensitivity to pH, ionic strength, and temperature. At low solution pH, high ionic strength, and low temperature, this hydrogel exhibited a low swelling ratio. The swelling ratio increased with the increase of pH, decreased ionic strength, and increased temperature. At a pH level above 8.3, the polyurethane became soluble in the water.

To study its capability for controlled drug delivery, the dye NBC and the protein lysozyme were employed. The study shows that at pH levels lower than 8.3, the compound's release rates increased with decreasing pH. As a pH level was increased higher than 8.3, the compounds were released with the dissolution of the PU matrix. Lysozyme release from the polyurethane hydrogel increases at higher ionic strengths. These results indicated that the release mechanism is a competitive ion exchange reaction among carboxyl groups, cationic compounds, and electrolytes in the solution through the electrostatic interaction.

The reversible pH sensitivity of the hydrogel was used for the scaffold fabrication by inkjet printing, which may be able to create spatially well defined drug releasing scaffolds out of this polymer. Our research demonstrates that this polymer is very versatile and may find many applications in the biomedical arena, such as the controlled release of drugs in response to the environmental stimuli and tissue engineering scaffolds.

Chapter 6

FUTURE DIRECTIONS

1. Encapsulation of the model drugs into the polyurethane scaffolds simultaneously during the printing on inkjet printer. The drug release behavior will then be studied to build up the relationship between the drug release in function of scaffold fabrication parameters such as scaffold shape, polymer concentration, drug concentration and environmental stimuli.
2. Fabrication of the polyurethane micro- or nano-sized spheres as drug carrier. The drug release behavior will be studied to build up the correlation among environmental pH, ionic strength, drug release and swelling.
3. Fabrication of the polyurethane scaffolds by electrospinning technique, and cell printing onto the scaffold for in-vitro attachment and proliferation study.

REFERENCES:

1. Ertel, S.I., Kohn, J., *Evaluation of a series of tyrosine-derived polycarbonates as degradable biomaterials.* J Biomed Mater Res, 1994. **28**(8): p. 919-30.
2. Sawhney, A.S., Hubbell, J. A., *Rapidly degraded terpolymers of dl-lactide, glycolide, and epsilon-caprolactone with increased hydrophilicity by copolymerization with polyethers.* J Biomed Mater Res, 1990. **24**(10): p. 1397-411.
3. Radder, A.M., Leenders, H., Van Blitterswijk, C. A., *Interface reactions to PEO/PBT copolymers (Polyactive) after implantation in cortical bone.* J Biomed Mater Res, 1994. **28**(2): p. 141-51.
4. Engelberg, I., Kohn, J., *Physico-mechanical properties of degradable polymers used in medical applications: a comparative study.* Biomaterials, 1991. **12**(3): p. 292-304.
5. Courtman DW, P.C., Kashef V, McComb D, Lee JM, Wilson GJ., *Development of a pericardial acellular matrix biomaterial: Biochemical and mechanical effects of cell extraction.* J Biomed Mater Res, 1994. **28**: p. 655-666.
6. Ma L, G.C., Mao Z, Zhou J, Shen J, Hu X, Han C., *Collagen/chitosan porous scaffolds with improved biostability for skin tissue engineering.* Biomaterials, 2003. **24**: p. 4833-4841.
7. Silver FH, P.G., *Cell growth on collagen: A review of tissue engineering using scaffolds containing extracellular matrix.* J Long Term Eff Med Implants, 1992. **2**: p. 67-80.
8. Aigner J, T.J., Hutzler P, Campoccia D, Pavesio A, Hammer C, Kastenbauer E, Naumann A., *Cartilage tissue engineering with novel nonwoven structured biomaterial based on hyaluronic acid benzyl ester.* J Biomed Mater Res, 1998. **42**: p. 172-181.
9. Heller J, N.S., Fritzinger BK, Roskos KV, *Controlled drug release from bioerodible hydrophobic ointments.* Biomaterials, 1990. **11**(235-237.).
10. Domb AJ., *Biodegradable polymers derived from amino acids.* Biomaterials, 1990. **11**(686-689).
11. Leong KW, D.A.P., Marletta M, Langer R., *Bioerodible polyanhydrides as drug-carrier matrices. II. Biocompatibility and chemical reactivity.* J Biomed Mater Res, 1986. **20**: p. 51-64.
12. Ambrosio AM, A.H., Katti DS, Laurencin CT., *Degradable polyphosphazene/poly(-hydroxyester) blends: Degradation studies.* Biomaterials, 2002. **23**: p. 1667-1672.
13. Nagaoka S, A.K., Okuyama Y, Kawakami H., *Interaction between fibroblast cells and fluorinated polyimide with nano-modified surface.* Int J Artif Organs, 2003. **26**: p. 339-345.
14. Risbud MV, B.R., *Polyamide 6 composite membranes: Properties and in vitro biocompatibility evaluation.* J Biomater Sci Polym Ed, 2001. **12**: p. 125-136.
15. Fromstein, J.D., Woodhouse, K. A., *Elastomeric biodegradable polyurethane blends for soft tissue applications.* J Biomater Sci Polym Ed, 2002. **13**(4): p. 391-406.

16. Van Minnen B, S.B., van Leeuwen MB, van Kooten TG, Bos RR., *A long-term in vitro biocompatibility study of a biodegradable polyurethane and its degradation products.* J Biomed Mater Res A, 2005. **76(2)**: p. 377-385.
17. Liu C, G.Y., Qian Z, Fan L, Li J, Chao G, Tu M, Jia W., *Hydrolytic degradation behavior of biodegradable polyetheresteramide-based polyurethane copolymers.* J Biomed Mater Res A, 2005. **75**: p. 465-471.
18. Van Minnen B, L.M., Stegenga B, Zuidema J, Hissink CE, van Kooten TG, Bos RR., *Short-term in vitro and in vivo biocompatibility of a biodegradable polyurethane foam based on 1,4-butanediisocyanate.* J Mater Sci Mater Med, 2005. **16**: p. 221-227.
19. Guan J, F.K., Sacks MS, Wagner WR., *Preparation and characterization of highly porous, biodegradable polyurethane scaffolds for soft tissue applications.* Biomaterials, 2005. **26**: p. 3961-3971.
20. Yang TF, C.W., Cherng JY, Shau MD., *Synthesis of novel biodegradable cationic polymer: N,N-diethylethylenediamine polyurethane as a gene carrier.* Biomacromolecules, 2004. **5**: p. 1926-1932.
21. Gorna K, G.S., *Preparation, degradation, and calcification of biodegradable polyurethane foams for bone graft substitutes.* J Biomed Mater Res A, 2003. **67**: p. 813-827.
22. Grad S, K.L., Gorna K, Gogolewski S, Alini M., *The use of biodegradable polyurethane scaffolds for cartilage tissue engineering: Potential and limitations.* Biomaterials, 2003. **24**: p. 5163-5171.
23. McDevitt TC, W.K., Hauschka SD, Murry CE, Stayton PS., *Spatially organized layers of cardiomyocytes on biodegradable polyurethane films for myocardial repair.* J Biomed Mater Res A, 2003. **66**: p. 586-595.
24. Galletti G, U.G., Farruggia F, Baccarini E, Biagi G, Gogolewski S., *Prevention of platelet aggregation by dietary polyunsaturated fatty acids in the biodegradable polyurethane vascular prosthesis: An experimental model in pigs.* Ital J Surg Sci, 1989. **19**: p. 121-130.
25. Zhang J, D.B., Beckman EJ, Hollinger JO., *A biodegradable polyurethane-ascorbic acid scaffold for bone tissue engineering.* J Biomed Mater Res A, 2003. **67**: p. 389-400.
26. Yang, M. and J.P. Santerre, *Utilization of quinolone drugs as monomers: characterization of the synthesis reaction products for poly(norfloxacin diisocyanatododecane polycaprolactone).* Biomacromolecules, 2001. **2**(1): p. 134-41.
27. Yang, T.F., et al., *Synthesis of novel biodegradable cationic polymer: N,N-diethylethylenediamine polyurethane as a gene carrier.* Biomacromolecules, 2004. **5**(5): p. 1926-32.
28. Cohen, I.K., Diegelman, R. F., Lindblad, W. J., *Wound healing : biochemical and clinical aspects*. 1st ed. 1992, Philadelphia: Saunders. xxv, 630.
29. Farso Nielsen F, K.T., Gogolewski S., *Biodegradable guide for bone regeneration. Polyurethane membranes tested in rabbit radius defects.* Acta Orthop Scand, 1992. **63**: p. 66-69.

30. Galletti G, G.S., Ussia G, Farruggia F., *Long-term patency of regenerated neoaortic wall following the implant of a fully biodegradable polyurethane prosthesis: Experimental lipid diet model in pigs.* Ann Vasc Surg, 1989. **3**: p. 236-243.
31. Pavlova M, D.M., *Biocompatible and biodegradable polyurethane polymers.* Biomaterials, 1993. **14**: p. 1024-1029.
32. Warrer K, K.T., Nyman S, Gogolewski S., *Guided tissue regeneration using biodegradable membranes of polylactic acid or polyurethane.* J Clin Periodontol, 1992. **9(9, Part 1)**: p. 633-640.
33. Ganta SR, P.N., Long P, Gassner R, Motta LF, Papworth GD, Stolz DB, Watkins SC, Agarwal S., *Vascularization and tissue infiltration of a biodegradable polyurethane matrix.* J Biomed Mater Res A, 2003. **64**: p. 242-248.
34. Vermette, P., *Biomedical applications of polyurethanes*. Tissue engineering intelligence unit ; 6. 2001, Georgetown, Tex. Austin, Tex.: Landes Bioscience; Eurekah.com. 273.
35. Lamba, N.M.K., et al., *Polyurethanes in biomedical applications*. 1998, Boca Raton: CRC Press. 277.
36. Cardy, R.H., *Carcinogenicity and chronic toxicity of 2,4-toluenediamine in F344 rats.* J Natl Cancer Inst, 1979. **62**(4): p. 1107-16.
37. Schoental, R., *Carcinogenic and chronic effects of 4,4'-diaminodiphenylmethane, an epoxyresin hardener.* Nature, 1968. **219**(5159): p. 1162-3.
38. Zhang, J.Y., et al., *A new peptide-based urethane polymer: synthesis, biodegradation, and potential to support cell growth in vitro.* Biomaterials, 2000. **21**(12): p. 1247-58.
39. Guan, J., et al., *Synthesis, characterization, and cytocompatibility of elastomeric, biodegradable poly(ester-urethane)ureas based on poly(caprolactone) and putrescine.* J Biomed Mater Res, 2002. **61**(3): p. 493-503.
40. Guan, J. and W.R. Wagner, *Synthesis, characterization and cytocompatibility of polyurethaneurea elastomers with designed elastase sensitivity.* Biomacromolecules, 2005. **6**(5): p. 2833-42.
41. Heijkants, R.G., et al., *Design, synthesis and properties of a degradable polyurethane scaffold for meniscus regeneration.* J Mater Sci Mater Med, 2004. **15**(4): p. 423-7.
42. Zhang, C., N. Zhang, and X. Wen, *Improving the elasticity and cytophilicity of biodegradable polyurethane by changing chain extender.* J Biomed Mater Res B Appl Biomater, 2006. **79**(2): p. 335-44.
43. Zhang, C., N. Zhang, and X. Wen, *Synthesis and characterization of biocompatible, degradable, light-curable, polyurethane-based elastic hydrogels.* J Biomed Mater Res A, 2007. **82**(3): p. 637-50.
44. Ganta, S.R., et al., *Vascularization and tissue infiltration of a biodegradable polyurethane matrix.* J Biomed Mater Res A, 2003. **64**(2): p. 242-8.
45. Zhang, J.Y., et al., *Synthesis, biodegradability, and biocompatibility of lysine diisocyanate-glucose polymers.* Tissue Eng, 2002. **8**(5): p. 771-85.

46. Skarja, G.A. and K.A. Woodhouse, *Synthesis and characterization of degradable polyurethane elastomers containing and amino acid-based chain extender.* J Biomater Sci Polym Ed, 1998. **9**(3): p. 271-95.
47. Fromstein, J.D. and K.A. Woodhouse, *Elastomeric biodegradable polyurethane blends for soft tissue applications.* J Biomater Sci Polym Ed, 2002. **13**(4): p. 391-406.
48. Stokes, K., R. McVenes, and J.M. Anderson, *Polyurethane elastomer biostability.* J Biomater Appl, 1995. **9**(4): p. 321-54.
49. Phillips, R.E., M.C. Smith, and R.J. Thoma, *Biomedical applications of polyurethanes: implications of failure mechanisms.* J Biomater Appl, 1988. **3**(2): p. 207-27.
50. Stokes, K. and K. Cobian, *Polyether polyurethanes for implantable pacemaker leads.* Biomaterials, 1982. **3**(4): p. 225-31.
51. Stokes, K., A. Coury, and P. Urbanski, *Autooxidative degradation of implanted polyether polyurethane devices.* J Biomater Appl, 1987. **1**(4): p. 411-48.
52. Smith, R., C. Oliver, and D.F. Williams, *The enzymatic degradation of polymers in vitro.* J Biomed Mater Res, 1987. **21**(8): p. 991-1003.
53. Santerre, J.P., et al., *Interactions of hydrolytic enzymes at an aqueous-polyurethane interface. Protein at interfaces II.* J Am Chem Soc, 1995. **352**: p. 70.
54. Wen. J., et al., *XPS study of surface composition of a segmented polyurethane block copolymer modified by PDMS end groups and its blends with phenoxy.* Macromolecules, 1997. **30**: p. 7206-13.
55. Marchant, R., et al., *In vivo biocompatibility studies. I. The cage implant system and a biodegradable hydrogel.* J Biomed Mater Res, 1983. **17**(2): p. 301-25.
56. Anderson, J.M., *Mechanisms of inflammation and infection with implanted devices.* Cardiovasc Pathol, 1993. **2**(3 Suppl): p. 33s-41s.
57. Kao, W.J., et al., *Role for interleukin-4 in foreign-body giant cell formation on a poly(etherurethane urea) in vivo.* J Biomed Mater Res, 1995. **29**(10): p. 1267-75.
58. Santerre, J.P., et al., *Understanding the biodegradation of polyurethanes: from classical implants to tissue engineering materials.* Biomaterials, 2005. **26**(35): p. 7457-70.
59. Kao, W.J., et al., *Theoretical analysis of in vivo macrophage adhesion and foreign body giant cell formation on strained poly(etherurethane urea) elastomers.* J Biomed Mater Res, 1994. **28**(7): p. 819-29.
60. Woo, G.L., et al., *Biological characterization of a novel biodegradable antimicrobial polymer synthesized with fluoroquinolones.* J Biomed Mater Res, 2002. **59**(1): p. 35-45.
61. Casas, J., et al., *In vitro modulation of macrophage phenotype and inhibition of polymer degradation by dexamethasone in a human macrophage/Fe/stress system.* J Biomed Mater Res, 1999. **46**(4): p. 475-84.
62. Sutherland, K., et al., *Degradation of biomaterials by phagocyte-derived oxidants.* J Clin Invest, 1993. **92**(5): p. 2360-7.
63. Sutherland, K., Mahoney, J. R., Coury, A. J., Eaton, J. W., *Degradation of biomaterials by phagocyte-derived oxidants.* J Clin Invest, 1993. **92**(5): p. 2360-7.

64. Kaplan, S.S., et al., *Mechanisms of biomaterial-induced superoxide release by neutrophils.* J Biomed Mater Res, 1994. **28**(3): p. 377-86.
65. Sundaram, S., et al., *Role of leucocytes in coagulation induced by artificial surfaces: investigation of expression of Mac-1, granulocyte elastase release and leucocyte adhesion on modified polyurethanes.* Biomaterials, 1996. **17**(10): p. 1041-7.
66. Labow, R.S., et al., *The effect of oxidation on the enzyme-catalyzed hydrolytic biodegradation of poly(urethane)s.* J Biomater Sci Polym Ed, 2002. **13**(6): p. 651-65.
67. Labow, R.S., E. Meek, and J.P. Santerre, *Hydrolytic degradation of poly(carbonate)-urethanes by monocyte-derived macrophages.* Biomaterials, 2001. **22**(22): p. 3025-33.
68. Shive, M.S., S.M. Hasan, and J.M. Anderson, *Shear stress effects on bacterial adhesion, leukocyte adhesion, and leukocyte oxidative capacity on a polyetherurethane.* J Biomed Mater Res, 1999. **46**(4): p. 511-9.
69. Nakaoka, R., T. Tsuchiya, and A. Nakamura, *Studies on the mechanisms of tumorigenesis induced by polyetherurethane in rats: production of superoxide, tumor necrosis factor, and interleukin 1 from macrophages cultured on different polyetherurethanes.* J Biomed Mater Res, 2000. **49**(1): p. 99-105.
70. Lamba, N.M., K.A. Woodhouse, and S.L. Cooper, *Polyurethanes in biomedical applications*. 1998, Boca Raton USA: CRC Press.
71. Patrick, V., et al., *Biomedical applications of polyurethanes*. 2001, Austin, TX: Landes Bioscience. 220-241.
72. Engelberg, I. and J. Kohn, *Physico-mechanical properties of degradable polymers used in medical applications: a comparative study.* Biomaterials, 1991. **12**(3): p. 292-304.
73. Ma, L., et al., *Collagen/chitosan porous scaffolds with improved biostability for skin tissue engineering.* Biomaterials, 2003. **24**(26): p. 4833-41.
74. Leong, K.W., B.C. Brott, and R. Langer, *Bioerodible polyanhydrides as drug-carrier matrices. I: Characterization, degradation, and release characteristics.* J Biomed Mater Res, 1985. **19**(8): p. 941-55.
75. Ambrosio, A.M., et al., *Degradable polyphosphazene/poly(alpha-hydroxyester) blends: degradation studies.* Biomaterials, 2002. **23**(7): p. 1667-72.
76. Gisselfalt, K., B. Edberg, and P. Flodin, *Synthesis and properties of degradable poly(urethane urea)s to be used for ligament reconstructions.* Biomacromolecules, 2002. **3**(5): p. 951-8.
77. Zhang, J., et al., *A biodegradable polyurethane-ascorbic acid scaffold for bone tissue engineering.* J Biomed Mater Res A, 2003. **67**(2): p. 389-400.
78. Chen, K.Y., J.F. Kuo, and C.Y. Chen, *Synthesis, characterization and platelet adhesion studies of novel ion-containing aliphatic polyurethanes.* Biomaterials, 2000. **21**(2): p. 161-71.
79. Silver, J.H., J.W. Marchant, and S.L. Cooper, *Effect of polyol type on the physical properties and thrombogenicity of sulfonate-containing polyurethanes.* J Biomed Mater Res, 1993. **27**(11): p. 1443-57.

80. Nojiri, C., et al., *In vitro studies of immobilized heparin and sulfonated polyurethane using epifluorescent video microscopy.* Asaio J, 1995. **41**(3): p. M389-94.
81. Silver, J.H., et al., *Anticoagulant effects of sulphonated polyurethanes.* Biomaterials, 1992. **13**(6): p. 339-44.
82. Yeong, W.Y., et al., *Rapid prototyping in tissue engineering: challenges and potential.* Trends Biotechnol, 2004. **22**(12): p. 643-52.
83. Yeong, W.Y., et al., *Comparison of drying methods in the fabrication of collagen scaffold via indirect rapid prototyping.* J Biomed Mater Res B Appl Biomater, 2007. **82**(1): p. 260-6.
84. Dhariwala, B., E. Hunt, and T. Boland, *Rapid prototyping of tissue-engineering constructs, using photopolymerizable hydrogels and stereolithography.* Tissue Eng, 2004. **10**(9-10): p. 1316-22.
85. Hollister, S.J., *Porous scaffold design for tissue engineering.* Nat Mater, 2005. **4**(7): p. 518-24.
86. Boland, T., et al., *Cell and organ printing 2: fusion of cell aggregates in three-dimensional gels.* Anat Rec A Discov Mol Cell Evol Biol, 2003. **272**(2): p. 497-502.
87. Yeong, W.Y., et al., *Indirect Fabrication of Collagen Scaffold Based on Inkjet Printing Technique.* Rapid Prototyping Journal, 2006. **12**(4): p. 229-237.
88. Boland, T., et al., *Application of inkjet printing to tissue engineering.* Biotechnol J, 2006. **1**(9): p. 910-7.
89. Varghese, D., et al., *Advances in tissue engineering: cell printing.* J Thorac Cardiovasc Surg, 2005. **129**(2): p. 470-2.
90. Boland, T., et al., *Rapid prototyping of artificial tissues and medical devices.* Advanced Materials and Processes, 2007. **165**(11): p. 51-53.
91. Xu, T., et al., *Viability and electrophysiology of neural cell structures generated by the inkjet printing method.* Biomaterials, 2006. **27**(19): p. 3580-8.
92. S. Khalil, J. Nam, and W. Sun, *Multi-nozzle deposition for construction of 3D biopolymer tissue scaffolds.* Rapid Prototyping Journal, 2005. **11**(1): p. 9-17.
93. Liu, C.Z., et al., *Novel 3D collagen scaffolds fabricated by indirect printing technique for tissue engineering.* J Biomed Mater Res B Appl Biomater, 2008. **85**(2): p. 519-28.
94. Fedorovich, N.E., et al., *Hydrogels as extracellular matrices for skeletal tissue engineering: state-of-the-art and novel application in organ printing.* Tissue Eng, 2007. **13**(8): p. 1905-25.
95. Wilson, W.C., Jr. and T. Boland, *Cell and organ printing 1: protein and cell printers.* Anat Rec A Discov Mol Cell Evol Biol, 2003. **272**(2): p. 491-6.
96. Jyoji, I., *Formation and reaction of polyenesulfonic acid. I. Reaction of polyethylene films with SO3.* Journal of Polymer Science Part A: Polymer Chemistry, 1988. **26**(1): p. 167-176.
97. Anders, F., O. Greger, and J. Per, *Ionic interactions and transport in a low-molecular-weight model polymer electrolyte.* The Journal of Chemical Physics, 1998. **108**(17): p. 7426-7433.

98. Okkema, A.Z., S.A. Visser, and S.L. Cooper, *Physical and blood-contacting properties of polyurethanes based on a sulfonic acid-containing diol chain extender.* J Biomed Mater Res, 1991. **25**(11): p. 1371-95.
99. Koberstein, J. and L. Leung, *Compression-molded polyurethane block copolymers. II. Evaluation of microphase compositions.* Macromolecules, 1992. **23**: p. 6205-6213.
100. Couchman, P., *Prediction of glass-transition temperature for compatible blends formed from homopolymers of arbitrary degree of polymerization. Compositional variation of glass-transition temperatures.* Macromolecules, 1980. **13**: p. 1272-1276.
101. Blasi, P., et al., *Plasticizing effect of water on poly(lactide-co-glycolide).* J Control Release, 2005. **108**(1): p. 1-9.
102. Dunn, M.G., P.N. Avasarala, and J.P. Zawadsky, *Optimization of extruded collagen fibers for ACL reconstruction.* J Biomed Mater Res, 1993. **27**(12): p. 1545-52.
103. Healy, K.E., et al., *Kinetics of bone cell organization and mineralization on materials with patterned surface chemistry.* Biomaterials, 1996. **17**(2): p. 195-208.
104. Clark, P., P. Connolly, and G.R. Moores, *Cell guidance by micropatterned adhesiveness in vitro.* J Cell Sci, 1992. **103 (Pt 1)**: p. 287-92.
105. Webb, K., V. Hlady, and P.A. Tresco, *Relative importance of surface wettability and charged functional groups on NIH 3T3 fibroblast attachment, spreading, and cytoskeletal organization.* J Biomed Mater Res, 1998. **41**(3): p. 422-30.
106. Kowalczynska, H.M. and M. Nowak-Wyrzykowska, *Modulation of adhesion, spreading and cytoskeleton organization of 3T3 fibroblasts by sulfonic groups present on polymer surfaces.* Cell Biol Int, 2003. **27**(2): p. 101-14.
107. Sefton, M.V., C.H. Gemmell, and M. Gorbet, B., *What really is blood compatibility?* J Biomater Sci Polymer Edn, 2000. **11**(11): p. 1165-1182.
108. Nojima, K., et al., *Material characterization of segmented polyether poly(urethane-urea-amide)s and its implication in blood compatibility.* Polymer, 1987. **28**: p. 1017-1024.
109. Takahara, A., et al., *Effect of hydrophilic soft segment side chains on the surface properties and blood compatibility of segmented poly(urethaneureas).* J Biomed Mater Res, 1991. **25**(9): p. 1095-118.
110. Kim, Y.H., et al., *Enhanced blood compatibility of polymers grafted by sulfonated PEO via a negative cilia concept.* Biomaterials, 2003. **24**(13): p. 2213-23.
111. Lelah, M.D., et al., *Physicochemical characterization and in vivo blood tolerability of cast and extruded Biomer.* J Biomed Mater Res, 1983. **17**(1): p. 1-22.
112. Mironov, V., et al., *Organ printing: computer-aided jet-based 3D tissue engineering.* Trends Biotechnol, 2003. **21**(4): p. 157-61.
113. Lee., K.Y. and D.J. Mooney, *Hydrogels for tissue engineering.* Chemical Reviews, 2001. **101**(101): p. 1869-80.

114. Hoffman, A.S., *Molecular bioengineering of biomaterials in the 1990s and beyond: a growing liaison of polymers with molecular biology.* Artif. Organs, 1992. **16**(1): p. 43-9.
115. McHugh, A.J., *The role of polymer membrane formation in sustained release drug delivery systems.* J. Control. Release, 2005. **109**(1-3): p. 211-21.
116. Determan, M.D., J.P. Cox, and S.K. Mallapragada, *Drug release from pH-responsive thermogelling pentablock copolymers.* J. Biomed. Mater. Res. A, 2007. **81**(2): p. 326-33.
117. Gumusderelioglu, M. and D. Kesgin, *Release kinetics of bovine serum albumin from pH-sensitive poly(vinyl ether) based hydrogels.* Int. J. Pharm., 2005. **288**(2): p. 273-9.
118. Zhang, R., et al., *A novel pH- and ionic-strength-sensitive carboxy methyl dextran hydrogel.* Biomaterials, 2005. **26**(22): p. 4677-83.
119. Zhang, X., D. Wu, and C.C. Chu, *Synthesis and characterization of partially biodegradable, temperature and pH sensitive Dex-MA/PNIPAAm hydrogels.* Biomaterials, 2004. **25**(19): p. 4719-30.
120. Jeong, B., Y.H. Bae, and S.W. Kim, *Drug release from biodegradable injectable thermosensitive hydrogel of PEG-PLGA-PEG triblock copolymers.* J. Control. Release, 2000. **63**(1-2): p. 155-63.
121. Kipper, M.J., et al., *Design of an injectable system based on bioerodible polyanhydride microspheres for sustained drug delivery.* Biomaterials, 2002. **23**(22): p. 4405-12.
122. Matsumoto, A., R. Yoshida, and K. Kataoka, *Glucose-responsive polymer gel bearing phenylborate derivative as a glucose-sensing moiety operating at the physiological pH.* Biomacromolecules, 2004. **5**(3): p. 1038-45.
123. Rosler, A., G.W. Vandermeulen, and H.A. Klok, *Advanced drug delivery devices via self-assembly of amphiphilic block copolymers.* Adv. Drug. Deliv. Rev., 2001. **53**(1): p. 95-108.
124. Chen, F.M., et al., *Novel glycidyl methacrylated dextran (Dex-GMA)/gelatin hydrogel scaffolds containing microspheres loaded with bone morphogenetic proteins: formulation and characteristics.* J. Control. Release, 2007. **118**(1): p. 65-77.
125. Lecomte, F., et al., *pH-sensitive polymer blends used as coating materials to control drug release from spherical beads: importance of the type of core.* Biomacromolecules, 2005. **6**(4): p. 2074-83.
126. Murata, Y., et al., *Drug release properties of a gel bead prepared with pectin and hydrolysate.* J. Control. Release, 2004. **95**(1): p. 61-6.
127. Varma, M.V., A.M. Kaushal, and S. Garg, *Influence of micro-environmental pH on the gel layer behavior and release of a basic drug from various hydrophilic matrices.* J. Control. Release, 2005. **103**(2): p. 499-510.
128. Chen, S.C., et al., *A novel pH-sensitive hydrogel composed of N,O-carboxymethyl chitosan and alginate cross-linked by genipin for protein drug delivery.* J. Control. Release, 2004. **96**(2): p. 285-300.

129. Alvarez-Lorenzo, C. and A. Concheiro, *Reversible adsorption by a pH- and temperature-sensitive acrylic hydrogel.* J. Control. Release, 2002. **80**(1-3): p. 247-57.
130. Lee, K.Y. and D.J. Mooney, *Hydrogels for tissue engineering.* Chem. Rev., 2001. **101**(7): p. 1869-79.
131. Boland, T., et al., *Cell and organ printing 2: fusion of cell aggregates in three-dimensional gels.* Anat. Rec. A. Discov. Mol. Cell. Evol. Biol., 2003. **272**(2): p. 497-502.
132. Wilson, W.C., Jr. and T. Boland, *Cell and organ printing 1: protein and cell printers.* Anat. Rec. A. Discov. Mol. Cell. Evol. Biol., 2003. **272**(2): p. 491-6.
133. Boland, T., et al., *Application of inkjet printing to tissue engineering.* J. Biotech., 2006. **1**(9): p. 910-7.
134. Varghese, D., et al., *Advances in tissue engineering: cell printing.* J. Thorac. Cardiovasc. Surg., 2005. **129**(2): p. 470-2.
135. Xu, T., et al., *Inkjet printing of viable mammalian cells.* Biomaterials, 2005. **26**(1): p. 93-9.
136. Xu, T., et al., *Construction of high-density bacterial colony arrays and patterns by the ink-jet method.* Biotechnol. Bioeng., 2004. **85**(1): p. 29-33.
137. Arshady, R., *Desk reference of functional polymers : syntheses and applications*. 1997, Washington, DC: American Chemical Society. xviii, 820.
138. Wiggins, M.J., et al., *Biodegradation of polyether polyurethane inner insulation in bipolar pacemaker leads.* J. Biomed. Mater. Res., 2001. **58**(3): p. 302-7.
139. Aigner, J., et al., *Cartilage tissue engineering with novel nonwoven structured biomaterial based on hyaluronic acid benzyl ester.* J. Biomed. Mater. Res., 1998. **42**(2): p. 172-81.
140. Risbud, M.V. and R.R. Bhonde, *Polyamide 6 composite membranes: properties and in vitro biocompatibility evaluation.* J. Biomater. Sci. Polym. Ed., 2001. **12**(1): p. 125-36.
141. Poussard, L., et al., *Hemocompatibilty of new ionic polyurethanes: influence of carboxylic group insertion modes.* Biomaterials, 2004. **25**(17): p. 3473-83.
142. Okkema, A.Z., S.A. Visser, and S.L. Cooper, *Physical and blood-contacting properties of polyurethanes based on a sulfonic acid-containing diol chain extender.* J. Biomed. Mater. Res., 1991. **25**(11): p. 1371-95.
143. Obaidat, A.A. and K. Park, *Characterization of protein release through glucose-sensitive hydrogel membranes.* Biomaterials, 1997. **18**(11): p. 801-6.
144. Nakamae, K., et al., *Synthesis and characterization of stimuli-sensitive hydrogels having a different length of ethylene glycol chains carrying phosphate groups: loading and release of lysozyme.* J. Biomater. Sci. Polym. Ed., 2004. **15**(11): p. 1435-46.
145. Anna, G., et al., *Squeezing hydrogels for controlled oral drug delivery.* J. Control. Release, 1995. **48**: p. 141-148.
146. Lisa, B.-P. and A.P. Nikolaos, *Solute and penetrant diffusion in swellable polymers. IX. The mechanisms of drug release from ph-sensitive swelling-controlled systems.* J. Control. Release, 1989. **8**(3): p. 267-274.

147. J, R. and T. Toyoichi, *Swelling of ionic gels: quantitative performance of the Donnan theory.* Macromolecules, 1984. **17**: p. 2916-2921.
148. Khare, A.R. and N.A. Peppas, *Swelling/deswelling of anionic copolymer gels.* Biomaterials, 1995. **16**(7): p. 559-67.
149. Helmlinger, G., et al., *Interstitial pH and pO2 gradients in solid tumors in vivo: high-resolution measurements reveal a lack of correlation.* Nat. Med., 1997. **3**(2): p. 177-82.
150. Lee, E.S., et al., *Tumor pH-responsive flower-like micelles of poly(L-lactic acid)-b-poly(ethylene glycol)-b-poly(L-histidine).* J. Control. Release, 2007. **123**(1): p. 19-26.